A Study of a Piezoelectric Energy Harvesting System Using Magnetorheological Fluids

by

Hayford Azangbebil

A thesis submitted to the

School of Graduate and Postdoctoral Studies in partial

fulfillment of the requirements for the degree of

Master of Applied Science in Mechanical Engineering

Department of Automotive, Mechanical and Manufacturing Engineering/ Faculty of Engineering and Applied Science

University of Ontario Institute of Technology (Ontario Tech University)

Oshawa, Ontario, Canada

August 2020

THESIS EXAMINATION INFORMATION

Submitted by: Hayford Azangbebil

Master of Applied Science in Mechanical Engineering

Thesis title: A study of a Piezoelectric Energy Harvesting Using Magnetorheological Fluids.

An oral defense of this thesis took place on July 28, 2020 in front of the following examining committee:

Examining Committee:

Chair of Examining Committee	Dr. Amirkianoosh Kiani
Research Supervisor	Dr. Martin Agelin-Chaab
Examining Committee Member	Dr. Ahmad Barari
Examining Committee Member	Dr. Dipal Patel
Thesis Examiner	Dr. Jaho Seo

The above committee determined that the thesis is acceptable in form and content and that a satisfactory knowledge of the field covered by the thesis was demonstrated by the candidate during an oral examination. A signed copy of the Certificate of Approval is available from the School of Graduate and Postdoctoral Studies.

ABSTRACT

This thesis reports the study of a piezoelectric energy harvesting system using a thin layer of magnetorheological fluid as a soft impact mechanism to enhance the frequency of the energy generator. Currently, the major bottleneck of vibration energy harvesting is the dynamic nature of vibrations in the environment which necessitates that vibration energy harvesters change their frequency to match that of the source. This work used the variable rheological properties of magnetorheological fluids to tune the frequency of a piezoelectric energy harvester. The study employed both numerical and experimental studies to investigate the effect of using the fluid in vibration energy harvesting. The results obtained show an increase in the output voltage and frequency of the device by 9.7% and 36%, respectively. For the first time, a soft impact frequency-increased piezoelectric energy harvesting system using magnetorheological fluid is studied in this thesis.

Keywords: Magnetorheological fluids; frequency amplification; spring force; Heaviside function; yield stress.

AUTHOR'S DECLARATION

I hereby declare that this thesis consists of original work of which I have authored. This is a true copy of the thesis, including any required final revisions, as accepted by my examiners.

I authorize the University of Ontario Institute of Technology (Ontario Tech University) to lend this thesis to other institutions or individuals for the purpose of scholarly research. I further authorize University of Ontario Institute of Technology (Ontario Tech University) to reproduce this thesis by photocopying or by other means, in total or in part, at the request of other institutions or individuals for the purpose of scholarly research. I understand that my thesis will be made electronically available to the public.

Hayford Azangbebil

STATEMENT OF CONTRIBUTIONS

I hereby certify that I am the sole author of this thesis and that a part of this thesis has been published in IEEE Sensor Journal. I have used standard referencing practices to acknowledge ideas, research techniques, or other materials that belong to others. Furthermore, I hereby certify that I am the sole source of the creative works and/or inventive knowledge described in this thesis.

ACKNOWLEDGMENTS

I would like to, first of all, thank the Almighty God for the wisdom and guidance throughout my studies and the implementation of this project.

Secondly, I express my profound gratitude to my supervisor, Dr. Martin Agelin-Chaab, for his guidance, support, constructive criticism, and the opportunity to further my studies. I extend my gratitude to Dr. Atef Mohany and Mohammed Alziadeh for allowing me to use the vibration shaker for my experimental work.

I would also like to extend my appreciation to my friends, Bismark Addo Binney and Sylvester Djokoto, who made Canada 'home away from home' for me and constantly encouraging me.

TABLE OF CONTENTS

LIST OF FIGURES

LIST OF TABLES

LIST OF ABBREVIATIONS AND SYMBOLS

Abbreviations

AC	Alternating current
DC	Direct current
ECU	Engine control unit
ER	Electrorheological fluid
HARKE	Human activity recognition from kinetic energy
HVAC	Heating, ventilation and air-conditioning
MAV	Micro-air vehicle
MEMS	Microelectromechanical systems
MIT	Massachusetts Institute of Technology
MLP	Perceptron neural network
MR	Magnetorheological fluid
Nd-Fe-B	Neodynum iron boron
PDAs	Personal digital assistants
PMN-PT	Lead magnesium niobate-lead titanate
PVDF	Polyvinylidene fluoride
PZT	Lead zirconate titanate
RF	Radio frequency
SDOF	Single degree of freedom
VDCu	Vibration damping control unit

Symbols

B	magnetic field densisty
C	constant of fluid dependent on carrier fluid
d_1	initial gap between MRF and beam
E_{sh}	shim layer modulus of elasticity
E_p	piezoelectric layer modulus of elasticity
h_m	height of magnet
H	magnetic field intensity
Φ	particle volume fraction
$\boldsymbol{\tau}$	yield/shear stress
$\dot{\boldsymbol{\gamma}}$	shear rate
G	material storage modulus
g	acceleration due to gravity
$\boldsymbol{F}$	force
$\boldsymbol{f_0}$	offset force
f_c	frictional force
$\boldsymbol{c_0}$	viscous damping coefficient
$\boldsymbol{k_1}$	stiffness of beam
$\boldsymbol{k_2}$	stiffness due to MR fluid
$\boldsymbol{c_1}$	damping coefficient of beam
$\boldsymbol{c_2}$	damping coefficient due to fluid
$\boldsymbol{C_p}$	piezoelectric plate capacitance
$\boldsymbol{\theta}$	piezoelectric coefficient
R	load resistance
$\boldsymbol{v}$	voltag**e**
$\boldsymbol{\omega}$	angular velocity
t	time

x	displacement
$\dot{\boldsymbol{x}}$	velocity
I	moment of inertia
$\boldsymbol{K_e}$	piezoelectric coupling coefficient
m	mass
η	plastic viscosity of fluid
K_{eff}	overall stiffness of beam
r	radius of magnet
l_b	free vibrating length of beam
w	width of beam
t_p	piezoelectric layer thickness
t_{sh}	shim layer thickness
μ_0	permeability of free space
ζ	damping ratio
φ	electromechanical conversion efficiency

Chapter 1: Introduction

1.1. Overview

Harvesting energy from the environment has generated profound interest from the scientific community and industry in the recent past. The growing interest in energy harvesting is attributed partly to the advancement of technology which has led to the production of electronic devices with milliwatts and microwatts power requirements. There is also the quest to find alternative sources of energy with little environmental impact. The purpose of energy harvesting from the environment is mostly to power small electronics and microelectromechanical systems (MEMS). Some of these devices include cart tracking devices, micro-switches, pacemakers, environmental condition monitoring devices, structural health monitoring devices, etc. The power requirements of some electronic devices that can be powered by harvesting energy from the environment are tabulated in Table 1.1:

Table 1.1 Power requirement of some electronic devices [1]

Device	Power Required (μW)
RFID tag	10
Sensors/remotes	100
Hearing aids	1 000
Bluetooth transceiver	10 000

As of 2005, the market for MEMS systems stood at US $8 billion and it is expected to grow up to US $200 billion in 2025 [2]. Normally, these small-power devices are powered by

batteries. However, batteries, by their nature, degrade with time and need replacement. There is also the issue of size, cost, and environmental impact of batteries. In some applications, MEMS devices are remotely located or placed in locations that are not accessible for routine maintenance and replacement. To minimize the bottlenecks associated with using batteries to power MEMS systems or microsensors, there is an impetus to design systems that can harness energy in their immediate environment to power themselves.

There are several forms of energy available in the environment that can be harvested to power wireless devices. Some of these include wind energy, which could be harvested using micro wind turbines; sound energy, using piezoelectric transducers; thermal energy based on the Seebeck effect, Peltier effect and Thomson effect using thermoelectric generators [3], [4]; electromagnetic radiations like radio-frequency waves, light waves, etc. and mechanical sources like vibration which is considered the most abundant in the environment. Mechanical energy is available in the environment in the form of vibrations in machine tools, industrial machines, and civil engineering structures. Even though vibration is ubiquitous in the environment, it is mostly randomly distributed and exists in the low-frequency domain (below 200 Hz). Various sources of vibration available in the environment are shown in Table 1.2 [5].

Table 1.2 Sources of vibration with their acceleration amplitudes and fundamental frequencies [5]

Source	Amplitude (m/s^2)	Frequency (Hz)
Clothes dryer	3.5	121
Car instrument panel	3	13
Car engine compartment	12	200
Blender casing	6.4	121
Small microwave oven	2.5	121
Person nervously tapping their heel	3	1
HVAC vents in office building	0.2-1.5	60
Windows next to a busy road	0.7	100
CD on notebook computer	0.6	75
Door frame just after door closes	3	125

Energy from vibration is mostly harvested using three conversion techniques. These include electrostatic, electromagnetic, and piezoelectric. Electrostatic converters consist of a dielectric medium sandwiched between two separate conductors with opposite charges. These charges establish an electric field between the plates/conductors. When there is relative motion between the plates, the energy stored in the electric field can be pushed into an external circuit. Electrostatic energy harvesters are easier to manufacture in the MEMS

scale, are inexpensive, sensitive to low-level vibrations [6], etc. Their major drawback is that they need an initial charge input or voltage to work.

Electromagnetic energy converters convert a changing magnetic field into voltage. This method is based on Faraday's law of electromagnetic induction which states that whenever there is a changing magnetic field in the vicinity of a coil, a voltage is induced in the coil. The magnitude of the induced voltage depends on the strength of the magnetic field, length of the coil, and how fast the coil is moved through the magnetic field. The basic requirement here is the existence of relative motion between the coil and the magnetic field. Electromagnetic energy converters are mostly used at the macro-scale. They have low voltage outputs when used at the micro-level because of the difficulty of fabricating micro-coils with a greater number of turns using thick and thin film deposition techniques [7].

Piezoelectric energy conversion is based on certain materials such as ceramics, microfiber materials, etc. that generate electric charges when they are squeezed. Piezoelectric energy conversion offers the highest power density among electromagnetic and electrostatic conversion and is easier to produce at the MEMS-scale level [8]. Piezoelectric energy harvesting has been studied extensively especially in the past decade but there remain some bottlenecks that need addressing. The major problem with energy harvesting from vibration currently is the variance in frequency of excitation which requires constant tracking by the generator to be able to harvest useful power. Piezoelectric energy conversion is the main focus of this thesis due to its advantages over the rest stated earlier.

1.2. Research Motivation and Objectives

Magnetorheological fluids are in a family of fluids collectively known as smart fluids. These undergo dramatic rheological changes in the presence of an external stimulus. Magnetorheological (MR) fluids add stiffness to the system and have been used in vibration suppression systems [9]–[12]. The ease with which the stiffness due to MR fluids is varied can be exploited in vibration energy harvesting using piezoelectric and electromagnetic conversion techniques. This is an important application area of MR fluids that is not well explored. It is worth mentioning that most of the energy conversion using MR fluids have been done using electromagnetic induction. Also, the current impact-based piezoelectric energy harvesting systems uses hard impact mechanisms. However, they generate high stresses in the beam which in addition to the bending stresses that can exceed the yield stress leading to mechanical failure.

The primary objective of this thesis is to investigate the potential of using magnetorheological fluid to enhance the energy harvesting potential of piezoelectric energy generators. More specifically, to study the use of a thin film MR fluid as a soft impact mechanism to enhance the frequency of a low-frequency piezoelectric energy harvester. The sub-objectives include:

i) Study the effect of using magnetorheological as an impact object for piezoelectric energy harvesting.

ii) Examine the effect of varying the magnetic field on the output voltage of the piezoelectric bimorph.

iii) Study the effect of the size of the magnet on the energy generator.

iv) Compare the theoretical and experimental results based on a simple mathematical model.

1.3. Thesis Outline

This thesis is divided into 5 chapters. Chapter 1 provides the background, motivation, and objectives of the study. Chapter 2 presents a review of the existing literature of the main concept to identify the state of the art and challenges that need to be addressed. Piezoelectric energy harvesting techniques and magnetorheological fluids will also be reviewed to identify potential applications and challenges. It will help provide context for readers and the basis for this thesis work. Chapter 3 presents the methodology employed in this study. Both the theoretical analysis and experimental methods to be used will be explained. In Chapter 4, a discussion of the theoretical and experimental results will be presented. Finally, Chapter 5 will report the conclusion and provide recommendations for future studies on this research.

Chapter 2: Literature Review

This chapter focuses on a review of existing literature on vibration energy harvesting. Magnetorheological devices with energy harvesting potential are also reviewed. Topics covered here include applications of piezoelectric energy harvesters, and energy harvesting or self-powered MR devices.

2.1. Application of Piezoelectric Energy Harvesting

Ever since the concept of harvesting waste energy from the environment gained more prominence in the scientific community, various self-powered devices have been fabricated both as ordinary prototypes and commercial products. These products include biomedical implants, wearable devices, and wireless sensors (for structural or equipment monitoring, corrosion detection, internet of Things (IoT), etc.) A self-powered wireless sensor that monitors corrosion in reinforced concrete structures has been reported in [13]. The device is powered by connecting two different meters immersed in an electrolyte. Piezoelectric energy harvesting systems have also been employed to detect failure or early cracks in mechanical or civil engineering structures [14]. These systems replace physical inspection of the structures for potential failure and routine maintenance procedures. In one of those systems reported by [15], two pairs of piezoelectric bimorph cantilever beams were mounted on a synchronous motor to harvest energy from the vibrations of the motor. The energy harvested was then used to power a microprocessor with data acquisition and communication functionalities. That system is equipped with sensors to monitor the state of the motor. The figure below shows the test rig of the motor with piezoelectric beams on top and side of the motor.

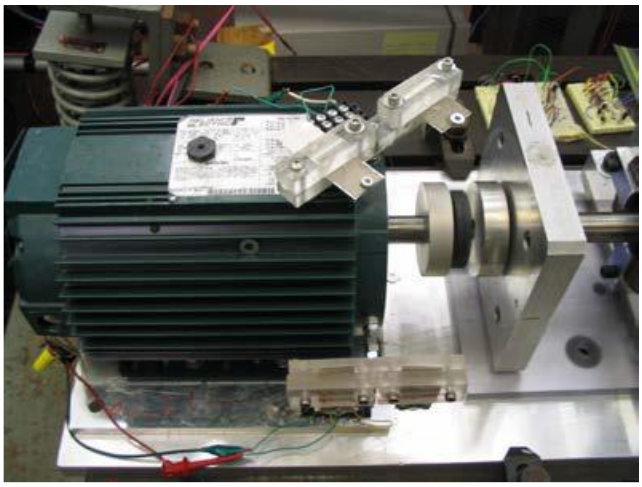

Figure 2.1 Photograph of the synchronous motor test rig with the piezoelectric cantilever beams mounted on top and sides of the motor [15]

Tomicek et al. [16] also designed a piezoelectric energy harvester to harvest energy from the seismic vibration of a building during earthquakes and, in turn, used the power to power sensors that gather data and report the potential presence of earthquakes. It is worth stating that such systems require a very high response time since most seismic vibrations are transient and whose intensity lasts only a few seconds. In their design, they used four harvesters connected in parallel to provide the amount of energy required to power the wireless sensor node for 5 seconds. The complete prototype design is shown in Fig. 2.2.

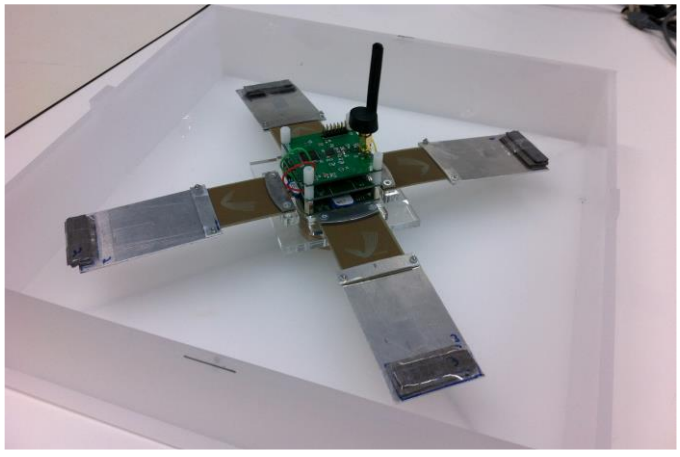

Figure 2.2 Assembled earthquake monitoring wireless sensor system [16]

Dondi et al. [17] also developed a self-powered wireless sensor to ensure the safety of operators manning industrial machinery with an attached trailer. The device consists of a tri-axial accelerometer and a tri-axial magnetometer to sense the trailer operating conditions. A wireless link is set up between the vehicle engine control unit (ECU) and embedded sensors to transmit data of the trailer to the vehicle stability controller. The harvester was a PZT cantilever beam with a resonant frequency of 112 Hz, and it is reported to be able to generate 23 μW to 850 μW from a baler vibration of $0.5g$ to $1g$.

A piezoelectric cymbal-like energy harvesting device with a diameter of 29 mm was integrated into asphalt to harvest the energy from the stress exerted on roads due to vehicular movement was presented by [18].

Monitoring traffic and the structural health of railways and road traffic tunnels have also been reported as an application area of ambient energy harvesting. The authors in [19] reported a piezoelectric energy generator with the required power conditioning interfaced circuit to power a microcontroller with radio frequency sensors.

An electromagnetic energy harvester, which consisted of a moving mass attached to a rigid bar and a motor connected to a mechanical gear part, was designed by [20] to harvest energy from stayed cable bridge, which could be used to power sensors that monitor the health state of the bridge. Maximum power of 15.46 mW was reported. The authors in [21] reported a performance-enhanced version of that reported in [8] by replacing the moving magnets and the fixed solenoid coil with a moving mass coupled to a rotational generator. They reported a higher power output of 35.67 mW. Figure 2.3 shows the proposed enhanced system.

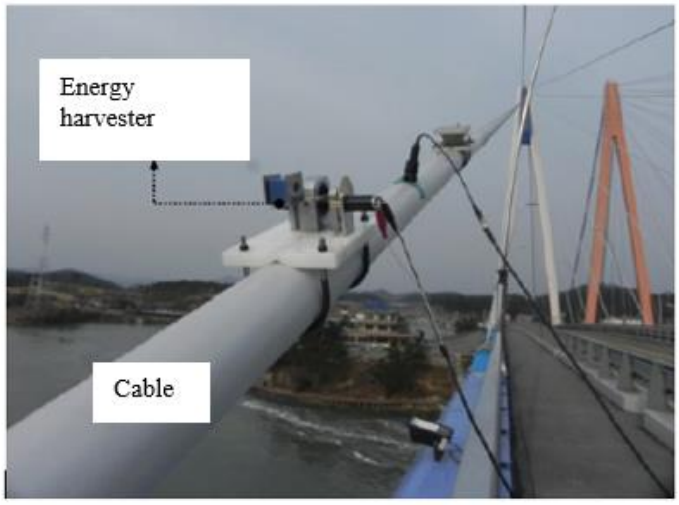

Figure 2.3 Proposed device installed on a stayed cable [21]

Also, Dumas et al. [22] developed, and validated a smart wireless sensor network for structural vibration damping and uncovering failure in airplane and helicopter structures. The device has the capability of harvesting waste energy from nearby regions of the structure and then use radio waves to transmit the data. Piezoelectric patches were attached to the structure and the electronic components placed above the patches. Failure in the structure is diagnosed using guided ultrasonic waves (also known as Lamb waves), that are created by a vibration-damping control unit (VDCu), while end-nodes acting as sensors are used to compare the signal with a reference signal that is stored in the memory. Each signal is then relayed to a central station that uses the signals from individual VDCus to assess the health of the structural zones being monitored. A neural network algorithm was used to examine the possibility of failure in the structure. Structural failure in any zone is determined by the neural network with a "Maintenance action" number between 0 and 1.

If the maintenance action is above 0.7, the failure is considered confirmed. With this value, the change in the structural response is lower than the reference value that was set.

Furthermore, the human body also constitutes an excellent area for the exploitation and application of energy harvesting. Normal human activities such as walking, running, breathing, muscle flexing, human body heat, etc. provide enough energy to power various wearable devices. Starner [23], one of the pioneers of harvesting energy from the human body to power wearables, reported that walking, body heat, and the movement of the upper limb produce a significant amount of energy as compared to breathing, blood pressure, and finger movement. Walking (heel strike) was reported to be the most potent and practical energy source. It is worth pointing out human-powered devices are readily available in the market today. Freeplay energy [24], has commercialized various human-powered devices such as flashlight lantern and radios. The radios produced by Freeplay energy use a mechanism that winds a spring around a spool, and when the spring is allowed to return to its original position, it drives DC generator to power the device. A simple hand cranking for about 30 seconds could power it for about an hour.

One of the most widely known human motion energy harvesters which are commercially built has been implemented in the Seiko Kinetic wrist-watches [25]-[26]. The kinetic motion energy harvester is implemented in a self-winding watch. The mechanical design is essentially an oscillating mass, called the rotor, which winds up a coil spring using a ratchet due to the movement of the wrist. The power stored in the spring is then used to drive the movement. The kinetic rotor serves as a gearbox with a ratio of 1:100, which can make a magnetic generator wheel spin at a higher speed. The generator coil then converts the changing magnetic field into electric power for operating a quartz movement. Similarly,

Applied Innovative Technologies [27] also produces human-powered flashlights that provide excellent illumination for five or more minutes when shaken for about 30 seconds. The shaking drives a magnet through a coil to generate power, which can be stored.

The application of human power in computing and communication systems has also received keen attention lately. Pagers, laptops, cell phones, and personal digital assistants (PDAs) are going battery-free or at least battery-assisted. Handheld rechargers and step-chargers are being used to power cellphones and even laptops. AladdinPower's rechargers have been reported to be able to power a cellphone up to 20 minutes by pumping a handheld device.

Moreover, harvesting energy from the human gait has been implemented in shoe inserts. One of the earliest shoe inserts energy harvesting devices was reported by [28] in MIT Media Lab. The said device was made by inserting piezoelectric materials in the sole of sneakers, and as the wearer walks, the mechanical stress exerted on the piezoelectric materials results in voltage generation. The prototype device that was built was used to power an RF tag. It is interesting to note that, the shoe could be used to power radios, navigation systems, night vision, toys, and detectors that can essentially warn soldiers of nearby land mines. A pictorial view of the device reported by the authors is shown below:

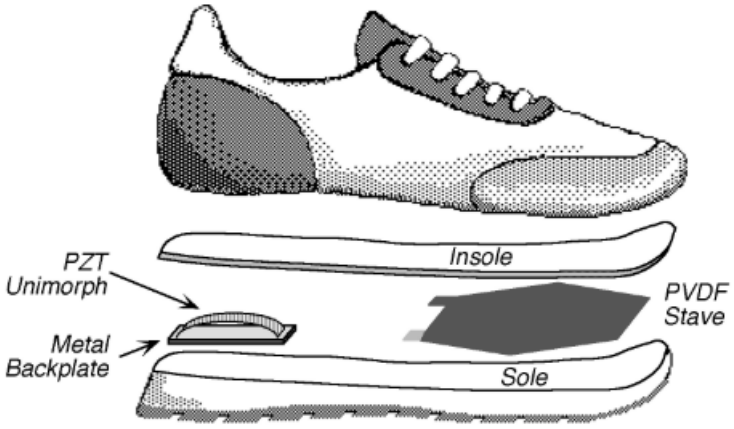

Figure 2.4 Exploded view showing the integration of the piezoelectric material [28]

Several other shoe energy harvesters have also been reported in the literature. Rocha et al. [29] also designed a shoe energy harvester using a combination of polyvinylidene fluoride (PVDF) polymers and an electrostatic harvester coupled to the sole of the shoe. The electrostatic harvester consisted of two metallic plates separated by foam, which changed its thickness when the person stepped on the floor. Xei and Cai [30] used an amplification mechanism to improve the energy harvesting efficiency of the shoe-mounted energy consisting of several piezoelectric bimorphs and sliders. They experimentally obtained 0.41 $mW\ cm^{-3}$. Jung et al. also used a flexible and curved piezoelectric material in a shoe insert to enhance the power output of the device. Experimental results yielded 25 V and 20 μA during normal walking by a 68 kg person. The authors in [31] designed a prototype insole-based piezoelectric energy harvesting device for human recognition during walking. They designed a sparse representation-based classification algorithm to leverage the voltage signals generated during walking for the user identification or verification. Data from 20 healthy people, each walking around 300 seconds were used to evaluate the performance of the human recognition system. The recognition accuracy grew up with an

increase in sampling rate but remained stable when the sampling rate was over 30Hz, meaning a minimum sampling rate of 30 Hz is required for the system to work effectively. Also, the verification accuracy was reported to be around 80% for both the piezoelectric energy harvesting signals from the front and rear of the insole, while it increased to about 90% with the two signals combined.

Granstrom et al. [32] developed an energy harvesting backpack to harvest energy from the differential forces between the wearer and backpack. The device was intended to be used by soldiers, emergency personnel, field workers, etc. to reduce the number of batteries they carry. Piezoelectric materials made of PVDF were used to replace the normal straps of the backpack. The energy harvesting backpack is shown below:

Figure 2.5 Schematic of the energy harvesting backpack with piezoelectric straps [32]

The introduction of smart biomedical devices has enhanced therapeutic and diagnostic methods to a greater extent. One major problem with implantable devices is the limited lifetime of batteries, which necessitate regular replacement. The replacement of these batteries requires rigorous surgical procedures, which could potentially put the patient at a higher risk. To confront the challenges associated with these devices, several researchers have investigated self-powered devices embedded in the human body. The authors in [33] presented a knee replacement device consisting of four piezoelectric ceramics in the tibia region of a knee implant. An average of 4.28 mW power was reported with an optimized device. A model of the instrumented knee implant is shown in Figure 2.6.

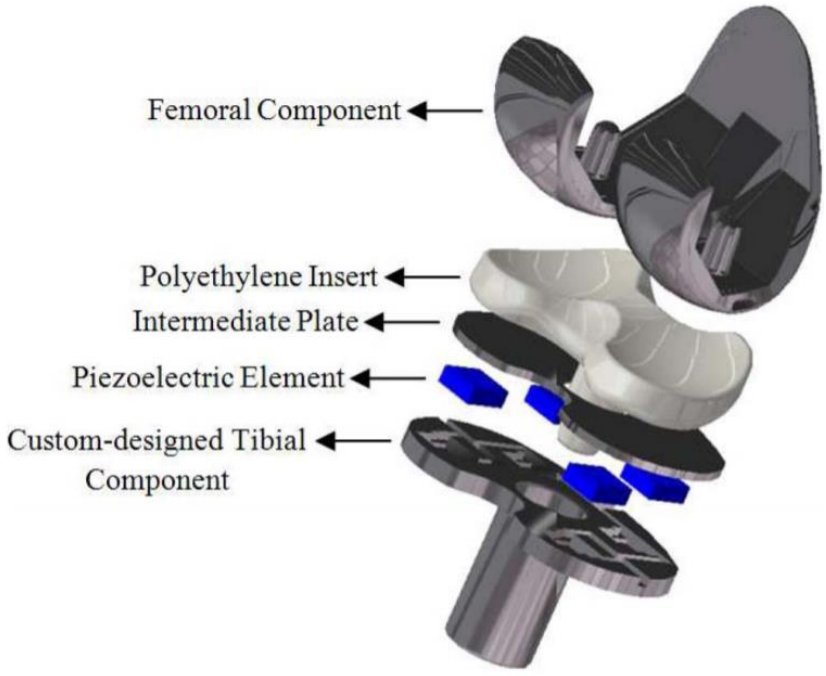

Figure 2.6 Model of the instrumented knee implant [33]

Holmberg et al. [34], carried out a study on a wireless self-powered sensor that was lodged in the tibial region of knee rehabilitation. The wireless device used a piezoelectric stack that offers the necessary energy for 6 capacitive force sensors. Based on results obtained

through experiments using a 55 kg person, it was shown that the piezoelectric device could generate 1.051 mJ of energy per step, which was adequate to drive the sensors, integrated signal processing circuits, along with wireless data transmitter with a low duty cycle. This system eliminates the need for the periodic painful medical procedure required to replace the batteries normally used in these devices

In addition to harvesting energy from people walking, Safaei et al. [35] introduced an instrumented knee replacement with 4 piezoelectric ceramics placed inside the bearing of the implant for sensing knee forces as well as contact locations. Test results of the device demonstrated that the energy produced during an hour of walking in typical conditions which was stored in a capacitor was adequate to provide power for nine minutes of sensing as well as data processing, and five seconds of wireless data transfer to a low power biomedical sensing circuit. The same authors presented an improved version of their previous device using 6 embedded piezoelectrics to measure compartmental forces as well as contact locations of the instrumented knee replacement.

Khalifa et al. [36] proposed a human activity recognition from kinetic energy harvesting (HARKE) device, which employed a piezoelectric energy harvester acting as both a power generator and a sensor for human activity recognition. The process is used to identify the type of human activity being undertaken from the energy harvester patterns without using any accelerometer, and it was reported to realize a saving of 79 % of the complete system power consumption.

In research done by Deterre et al. [37], a piezoelectric energy harvester was designed, fabricated, and tested for power generation from regular blood pressure variations to power up a leadless pacemaker (shown in Figure 7). The unit was a microfabricated spiral-shaped

piezoelectric beam within a flexible packaging equipped with a 10 μm diaphragm. The harvester had a diameter of 6 mm along with a volume of 21 mm^3. Results obtained from the experimental setup showed a power density of 3 $\mu J\ cm^{-3}$ per heartbeat. A conversion efficiency of 5.7×10^{-3} was reported for an optimum design operating at 1.5 Hz.

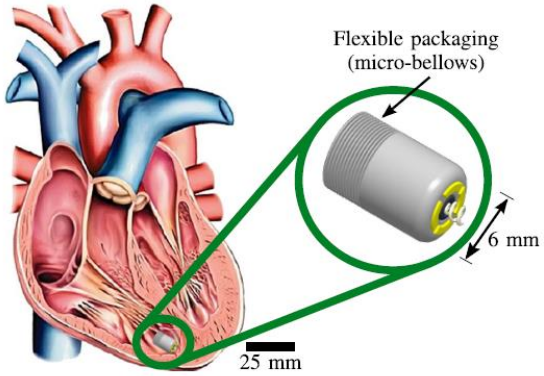

Figure 2.7 Schematic of an implantable leadless device embedded within a heart cavity with a deformable micro-bellows packaging [37]

Using a nonlinear piezoelectric energy harvester to drive pacemakers, Karami, and Inman [38] studied powering pacemakers by harvesting energy from the heartbeat's vibration. They used data presented in the literature to carry simulations and the results obtained indicated a nonlinear beam with dimensions $27 \times 27 \times 0.080\ mm^3$ could produce more than 3 μW of power for heartbeats ranging from 7 beats per minute to 700 beats per minute. Also, Hwang et al [39] used a pliant single-crystalline lead magnesium niobate-lead titanate (PMN-PT) piezoelectric power harvester for the creation of a self-powered cardiac pacemaker. Using PMN-PT with a high piezoelectric charge constant of $d_{33} = 2500\ pC\ N^{-1}$ (which is higher than that of PZT and $BaTiO_3$), they tested the device in a live rat's cardiac muscle and it was reported to have shown a pretty high output current of 0.223 mA along with an output voltage of 8.2 V. PMN-PT offers better

performance than the mostly widely used PZT. However, they are mostly costly, suffer more from fatigue and they also suffer temperarure instability.

Other studies have been done to ascertain the feasibility of harvesting energy from avian sources. Study on flying insects as hosts embedded with electronic devices, for the development of cyborg micro-air vehicles (MAV), used for autonomous surveillance and reconnaissance vehicles was presented by [40]. Shafer et al. [41] investigated the potential ofbirdsasasourceofenergytopowerwildlifetracking tags. The flapping frequenciesof birds in a flight tunnel test were measured (from11.5 to 14.5 Hz) and the magnitude of the acceleration of the birds in the flight was reported to be in the range of 1.5-1.75 g. The same group of researchers introduced energy harvesting from marine animals based on fluid flow or pressure gradients as the animal dives [42]. This could prolong the tracking tags that gather information about the movement of the animals.

2.2. Piezoelectric Energy Harvesting Materials

Piezoelectric energy harvesters exploit the potential of piezoelectric materials to generate electric potential upon the application of mechanical stress. The inverse phenomenon involves converting electric potential into mechanical displacement or force. The direct piezoelectric effect was first reported by the Curie brothers (Pierre and Jacques) in1880. They observed that when quartz or tourmaline crystals were squeezed, they produced electric charges. Piezoelectric materials can occur naturally, such as tourmaline, quartz, topaz, cane sugar, dry bone, and Rochelle salt. [43]. The indirect effect was observed by Lippmann in 1881 using thermodynamic theory [44]. Currently, the most common and high performing piezoelectric materials such as lead zirconate titanate (PZT), barium

titanate, polyvinylidene fluoride (PVDF), active and micro-fiber composites are artificially produced. Piezoelectricity is a coupled phenomenon between the electrical domain and the mechanical domain. The following constitutive equations link the mechanical parameters (stress and strain) to the electrical parameters (charge density and electric field):

$$\{S\} = [s^E]\{T\} + [d]\{E\} \quad (2.1)$$

$$\{D\} = [d]\{T\} + [\varepsilon^T]\{E\} \quad (2.2)$$

Where, $[d]$ is the piezoelectric coupling coefficient matrix which provides the mechanism for the power generation in energy harvesting, $[s^E]$ is the compliance matrix at the constant electric field, $\{T\}$ is the mechanical field, $\{E\}$ is the electric field strength, $\{D\}$ is charge density or electric displacement and $[\varepsilon^T]$ is the permittivity matrix at constant stress. Piezoelectric materials are mostly operated in two modes, namely, 33 or 31-mode depending on the direction of the application of the mechanical force or electric voltage. In the 33-mode, both the voltage and the force are in the same direction while in the 31-mode, the voltage is applied in the 3-direction and the force in the 1-direction. The 33-mode is normally used in stack actuators, whereas the 31-mode is mostly used in piezoelectric bimorphs [45].

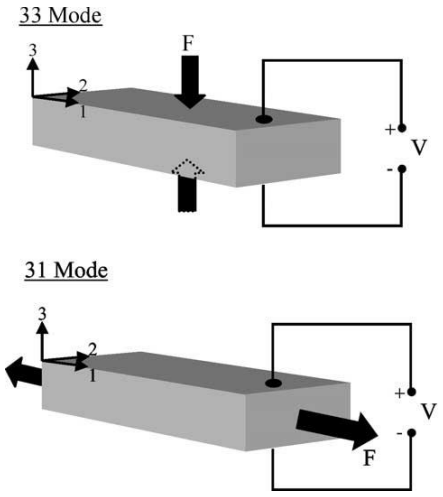

Figure 2.8 Modes of operation of piezoelectric materials [5]

2.3. Advances in Piezoelectric Energy Harvesting

Harvesting energy from the environment is an excellent yet challenging process in most cases because the energy available in the environment in the form of vibrations is most stochastic. Thus, vibration levels in most machinery, structures, and even human beings are randomly distributed with different frequencies. Typical vibration energy harvesters operate based on resonance. Therefore, there is always a mismatch between the frequency of the harvester and the source, which is dynamic. Vibration energy transducers, in general, produce maximum power only at resonance. This is a serious limitation because the frequency of natural vibrations is not constant, and therefore requires constant adjustment of the frequency of the harvester to match with that of the vibration source. Designing a system with a single optimum frequency is considered inefficient because this frequency depends on the mechanical and electrical characteristics of the device. These conditions are subject to change due to manufacturing tolerances or operating conditions such as temperatures or vibration amplitudes [46]. Vibration energy harvesters, therefore, require

tunability to match the dynamic excitation frequencies to produce useful energy if significant implementation of autonomous devices is to be achieved. Frequency tuning is based on the fundamental resonant frequency of a spring, mass, and damper system represented by [47]:

$$f_r = \frac{1}{2\pi}\sqrt{\frac{k}{m}} \tag{2.3}$$

Where *k* represents the spring constant, and *m* is the mass of the system. The spring constant of the energy harvester, however, is a function of the material properties of the harvester and its dimensions. For a cantilever-based harvester with a tip mass, the resonant frequency is also given by [48]:

$$f_r = \frac{1}{2\pi}\sqrt{\frac{Ywh^3}{4l^3(m+0.24m_b)}} \tag{2.4}$$

Where Y denotes Young's modulus of the beam material; l, w, and h are the length, width, and thickness of the beam, respectively; and m_b is the mass of the beam. Equation (2.4) clearly shows that the frequency of the generator can be altered by varying any of the parameters of that equation. However, in practice, it is difficult to alter the frequency of the generator by changing either the width or height [47].

Various studies have proposed different frequency tuning techniques of maximizing the power that can be harvested.

A novel frequency tuning technique was patented by [49]. The device uses a slider, which is controlled by an actuator to alter the vibrating length of the cantilever beam and hence the resonant frequency. The patented device is shown below:

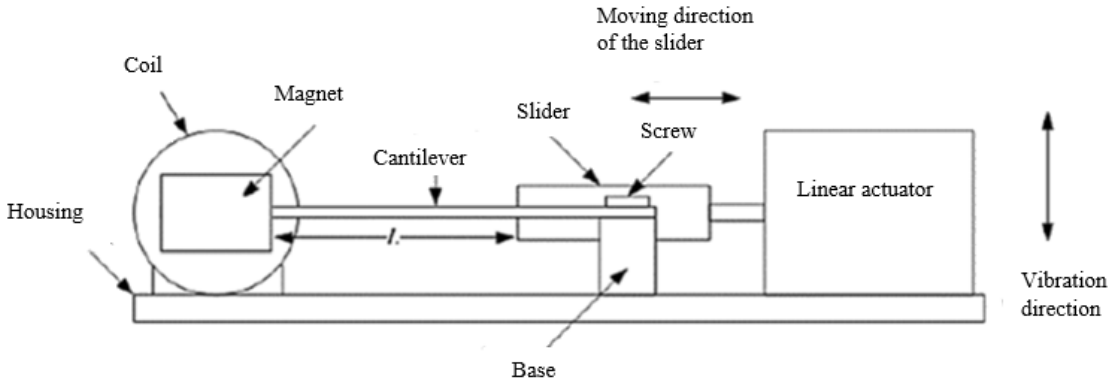

Figure 2.9 Adjustable vibration energy harvesting device [49]

Since it is impossible to vary the effective mass of the resonant cantilever beam, the authors in [50] devised a novel technique of changing the frequency of a piezoelectric cantilever beam with a tip-mass by adjusting the center of gravity of the tip mass. When the center of gravity of the tip mass is altered, additional torque is added to the system. Thus, the effective spring constant is changed. A schematic of the proposed technique is shown in Figure 2.10. They also deduced an approximate formula for the resonant frequency giving by Equation (2.5). The major difficulty with this design is its complexity. The authors demonstrated the concept using a rectangular beam which will be very difficulty to replicate in other cantilever architectures.

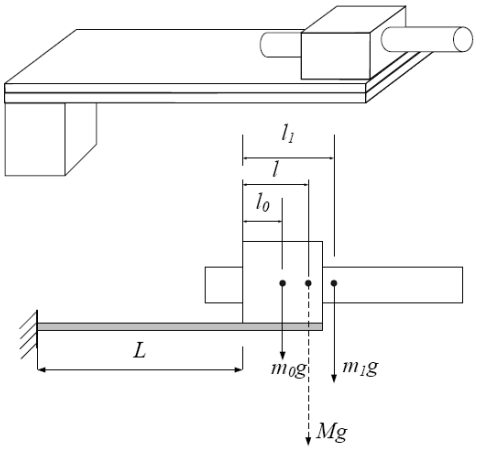

Figure 2.10 Schematic of the frequency tuning

$$f_r = \frac{1}{2\pi}\sqrt{\frac{Ywh^3}{12ml^3)}}\frac{6j^2+6j+2}{8j^4+14j^3+10.5j^2+4j+\frac{2}{3}} \quad (2.5)$$

Where $j = \frac{l}{L}$ (as shown in Figure 2.10).

Furthermore, Challa et al [51] designed and tested a bidirectional frequency tuning device using magnets. A piezoelectric beam with a resonant frequency of 26 Hz was successfully tuned over a frequency range of 22-32 Hz by applying a repulsive and an attractive magnetic force to the beam. With this technique, the resonant frequency can be tuned down or up using an attractive or a repulsive force, respectively. The device was able to output power of $240 - 280\ \mu W$ over the reported frequency range.The use of four magnets makes the device bulky. Also, the damping coefficient of the system increased by 71 % which led to power reduction. A schematic of the proposed device is shown in Figure 2.11.

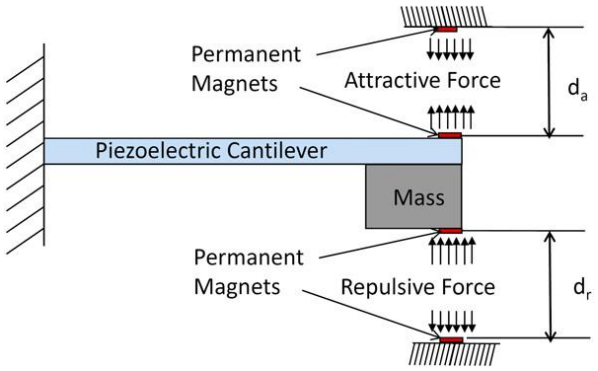

Figure 2.11 Schematic of the bidirectional frequency tuning device [51]

A technique of tuning the vibrating frequency of a piezoelectric beam using an axial preload was presented by [52]. It comprises a mechanical bolt operating through the main metal covering and repaired at the left-hand side edge wall. A capped stiff metal plate was connected to the bolt at the free end of the cantilever. When the bolt is turned clockwise, a compressive preload is applied on the beam while an anticlockwise turn creates a force to push the capping plate to the right-hand side, which can produce a tensile preload on the bimorph. A compressive preload applied to the piezoelectric beam was reported to have altered its frequency from 380 to 292 Hz. A different experiment conducted on a harvester with stiffened arms tuned the frequency from 440 to 460 Hz when a tensile preload was applied. The magnitude of forces used to tune the device was too high for a micro-device. For example, it was reported that a total force of 22.75 N was applied to the wings to achieve a resonance frequency shift of 22 %. The proposed device is shown.

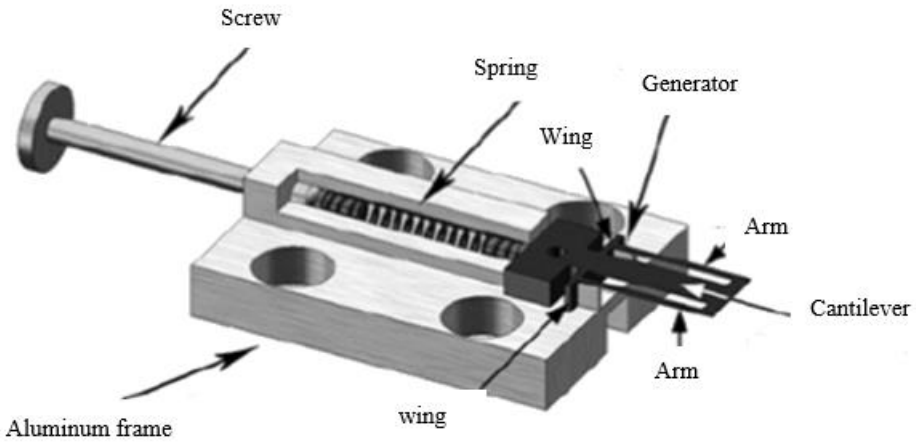

Figure 2.12 Schematic diagram of the proposed device by applying a mechanical preload [52]

Resonant frequency tuning has a serious defect as it can only tune the generator to a single frequency at a time. To overcome this challenge, different authors have proposed widening the operational bandwidth of the energy harvester. In one of such methods reported by Shahruz [53], a device that consisted of different cantilever beams with different lengths and masses was reported. With this technique, each cantilever beam with its tip mass is a generator with a specific resonant frequency. It is worth noting that the major disadvantage of this technique is that, at any instance, only one generator is likely to produce useful energy. Thus, it is inefficient, and it also has a low power density. A schematic of the reported device is shown below.

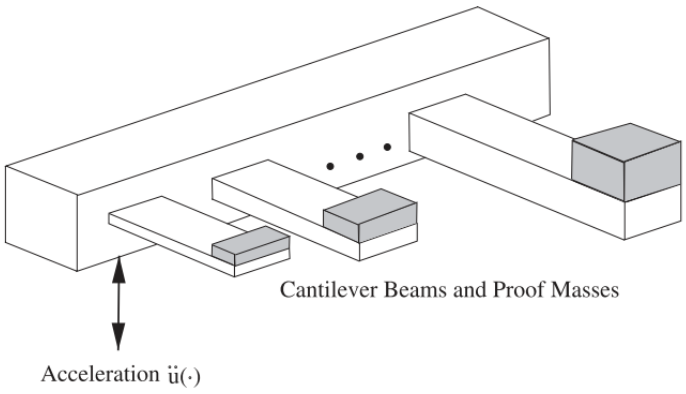

Figure 2.13 An array of piezoelectric generators [53]

Zhou et al. [54] also investigated piezoelectric energy harvester with coupled magnets to widen the operational bandwidth of the device. By altering the orientation of two external magnets, a broadband frequency response was achieved. This type of harvester leverages the nonlinear effects of the magnets to broaden the operational bandwidth of the device. The magnetic force of the magnets increases or decreases the stiffness of the cantilever depending on the polarities of the magnets interacting with each other. The device reported was said to be able to operate with a low, broad frequency range of 4-22 Hz. The concept is illustrated in the schematic below.

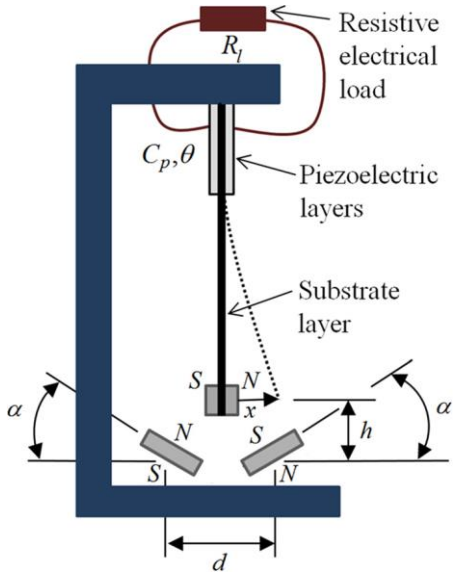

Figure 2.14 Schematic of broadband energy harvester with rotary magnets [54]

Furthermore, to overcome the challenges with harvesting energy from low-frequency vibrations, some authors have investigated frequency amplification techniques that convert vibrations with low-frequency to high-frequency vibrations. This technique is known to increase the efficiency of the harvester and also broaden its bandwidth. The inventors of this technique used a piezoelectric generator that converted the impact of a steel ball bouncing on a piezoelectric membrane into electrical energy [55]. Also, Halim et al. [56] studied a frequency up-conversion piezoelectric energy harvester for the human motion-related environment. In their work, they used a flexible driving beam with a tip mass and had dimensions of $58 \times 4.8 \times 1\ mm^3$ and two piezoelectric generating beams attached to a styrene support and had dimensions $15 \times 3.5 \times 0.8\ mm^3$ each. The device was reported to have generated 93.2 μW across a resistive load of 200 KΩ under 4 ms^{-2} acceleration. This technique is meant to reduce the mechanical damping ratio, but the piezoelectric beam is susceptible to failure due to the hard impact. The geometry of the device is shown below:

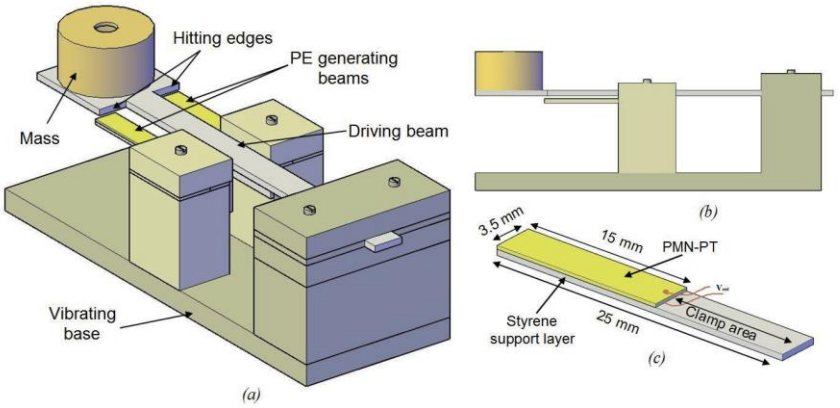

Figure 2.15 Bird's-eye view (a), side view (b), and piezoelectric generating beam with a plastic support layer (c) of the proposed frequency increased piezoelectric vibration energy harvester [57]

Moss et al [58] studied a vibro-impact energy harvester using two symmetric double-sided piezoelectric bimorph stops as the impact mechanism. The device is reported to have generated a power of 5.3 mW when it operated in the frequency range of 100-113 Hz from a host vibration of $0.45\ g$.

Zhang et al. [59] studied a novel impact-based frequency up-conversion with tunability using a rope-driven hybrid mechanism. They studied the effect of the rope margin on the frequency tuning of the piezoelectric energy harvester. Using numerical simulation and experimentation, the authors were able to show that the working frequency of the device could be changed from 74.75 to 106 Hz by adjusting the rope length from 0.5 mm to 2 mm without any need for structural re-fabrication of the device. It is worth pointing out the main focus of their work was to investigate the effect of the rope-margin on the central frequency of the proposed system. The numerical study was carried out by modeling the system as a piece-wise mas-spring-damper. The proposed system is shown in

Fig. 2.16:

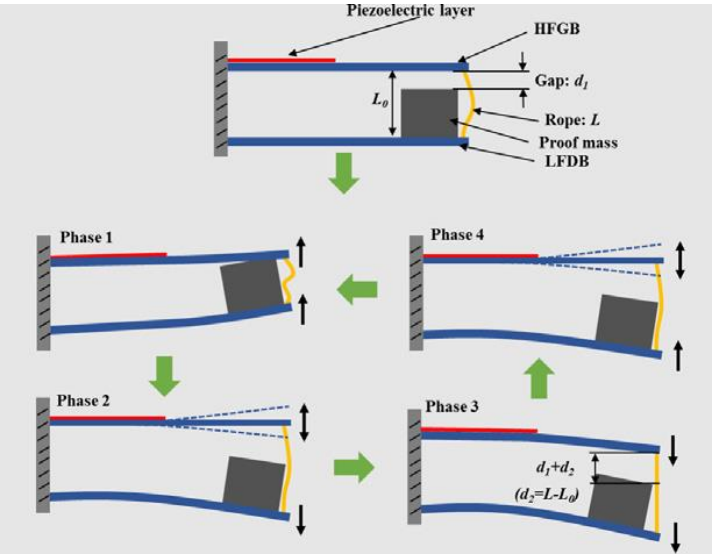

Figure 2.16 Schematic using the operation of the proposed frequency tunable device [59]

A piezoelectric energy harvester with a wide frequency response using mechanical stoppers as impact objects was microfabricated and reported by [60]. The device reported consisted of two MEMS piezoelectric PZT cantilevers arranged face-to-face. An impact-driven frequency increased device was also investigated by [61]. The device consisted of a low-frequency resonator, which is impacted by a high-frequency resonator. In their work, the high low-frequency beam acts as the driver of the high-frequency beam by transferring its energy to it during the impact. These systems use hard impact which makes the piezoelectric device more susceptible to fatigue and failure due to high stresses generated during the impact. These stresses can exceed the yield stress of the device causing failure

.

2.4. Magnetorheological Fluids

Magnetorheological fluids (or MR fluids) are part of a group of smart fluids whose rheological properties depend on the strength of an applied electrical or magnetic field. This group is made up of ferrofluids, electrorheological fluids (ER), and magnetorheological fluids (MR). Ferrofluids [62] are colloidal suspensions of magnetic particles with sizes smaller than 10 nm (usually made of magnetite) suspending in a carrier liquid such as water, hydrocarbons, esters, etc. When placed in the vicinity of a magnetic field, the viscosity of these fluids increases. The increase in viscosity is directly related to the intensity of the magnetic field.

Ever since Jacob Rabinov and Willis Winslow discovered magnetorheological fluid effect and electrorheological fluid effect, respectively, and almost concurrently [63]–[65], there have been many resurgences in research and development in magnetorheological fluids in the current decade. This has led to the development of devices like valves, mounts, and dampers. The fluid consists of magnetic particles (such as pure iron, carbonyl iron, or cobalt powder) and a carrier fluid. The carrier fluid is a non-magnetic, organic, or aqueous liquid and it is usually either silicone or mineral oil [66]. Upon the application of the magnetic field, the magnetizable particles acquire a dipole moment which aligns with the external magnetic field and forms chain-like structures. The formation of these chains induces reversible yield stress in the fluid [66]. This phenomenon is illustrated in Fig 2.17.

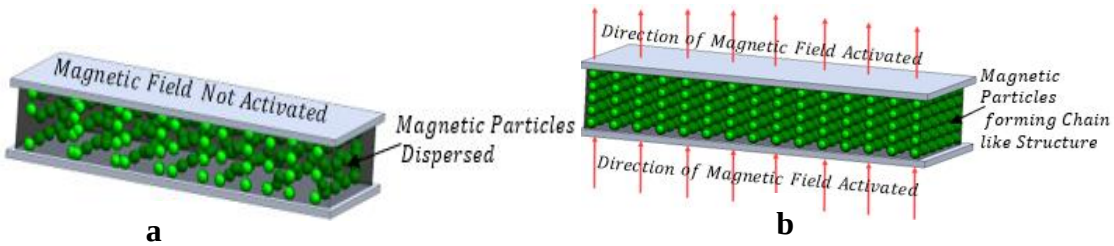

Figure 2.17 (a) Non-activated and (b) activated MR fluid [67]

Electrorheological fluids are energized with an electric field. ER fluids are made up of a special type of suspensions containing semi-conducting or polarizable materials acting as electro-responsive parts [68]. MR fluids are distinguished from ER fluids, mainly by the type of stimulus used to activate them. The major advantage of MR fluids over ER fluids is that they do not need high voltage to set up the field to activate them as is the case with ER fluids. This certainly obviates the need for high voltage to produce enough damping force. MR fluids, however, tend to saturate beyond certain field strength. This is depicted below:

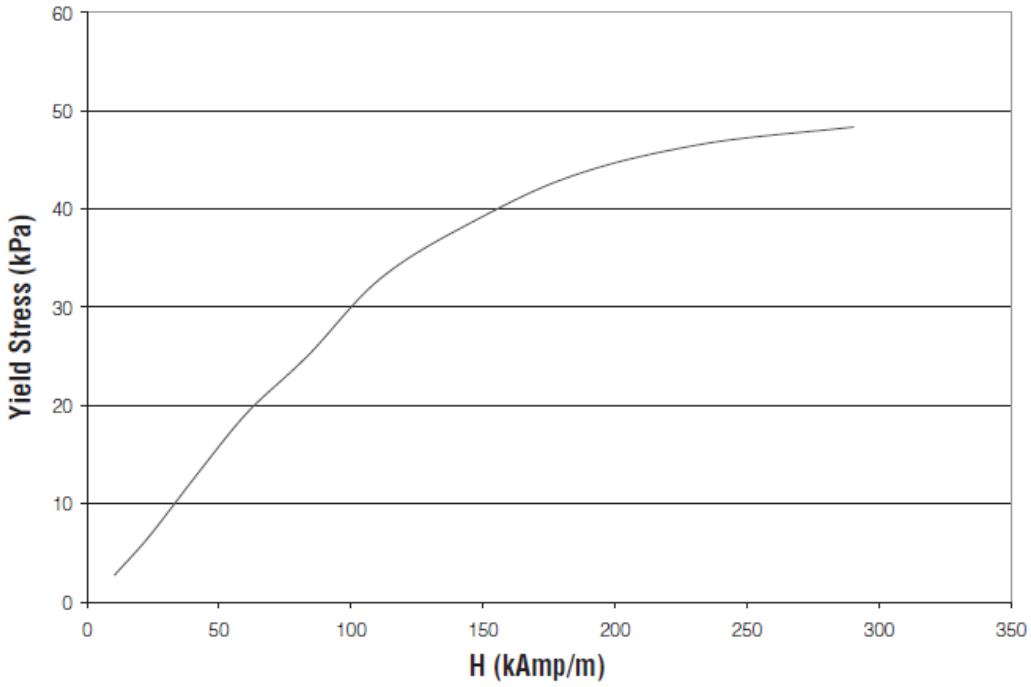

Figure 2.18 Yield stress vs magnetic field strength [69]

2.4.1. Different operational modes of MR fluids

Current MR fluids devices are designed based on three different operational modes, such as shear, squeeze, and valve mode. However, Goncalves and Carlson [70] recently proposed a new working mode known as magnetic gradient pinch mode. MR devices can work on any of the operational modes or a combination of them.

(a) As can be seen from Fig.. 2.19a, valve mode is when the fluid flow between two static structures. The flow is basically due to pressure gradients. This pressure difference is what is exploited and used in devices such as servo-valves, dampers, shock absorbers, and actuators [71]. Valve mode is the most commonly used mode.

(b) In shear mode, there is a relative motion between the plates, and this creates shear stress on the fluid. Examples of shear mode devices include clutches, brakes, chucking and locking devices, dampers, and structural composites.

(c) In the squeeze mode, the fluid is squeezed between two plates such that it flows radially. This model generates the highest yield stress [72], yet it has only been used in small amplitude vibration and impact dampers. There are two forms of squeeze mode: constant volume and constant contact area [73].

(d) In the pinched mode, the fluid flow through channels just like the valve, but the magnetic field is applied somewhat parallel to the direction of flow by arranging the poles axially along the flow direction and separating them by a non-magnetic spacer [74].

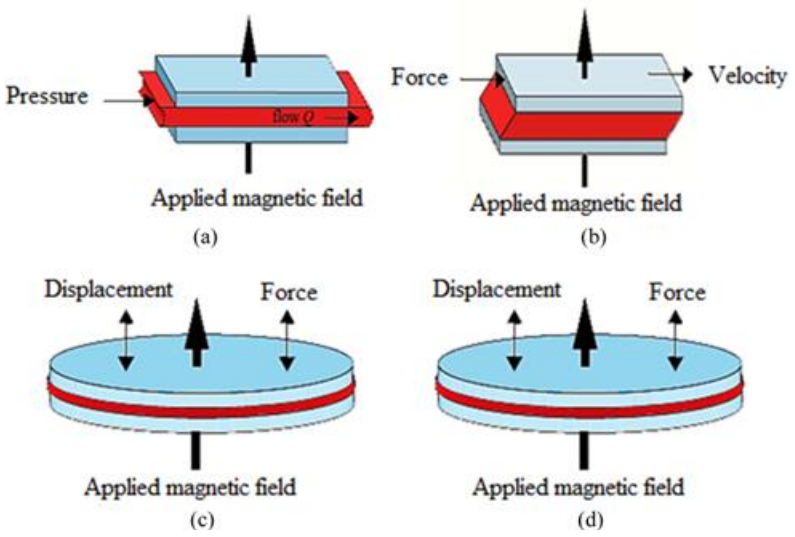

Figure 2.19 (a) Valve mode [75] (b) direct shear mode [76] (c) squeeze mode [77] and (d) magnetic gradient mode [70]

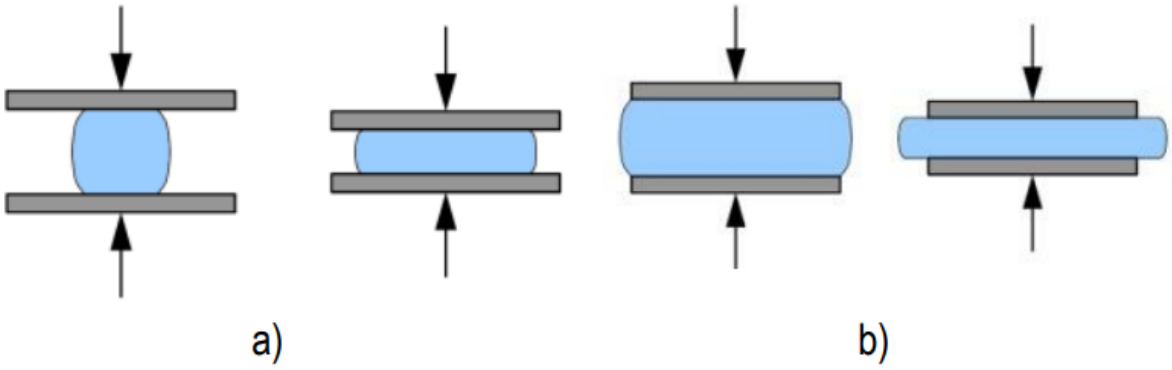

Figure 2.20 Forms of squeeze mode (a) constant volume (b) constant contact area [73]

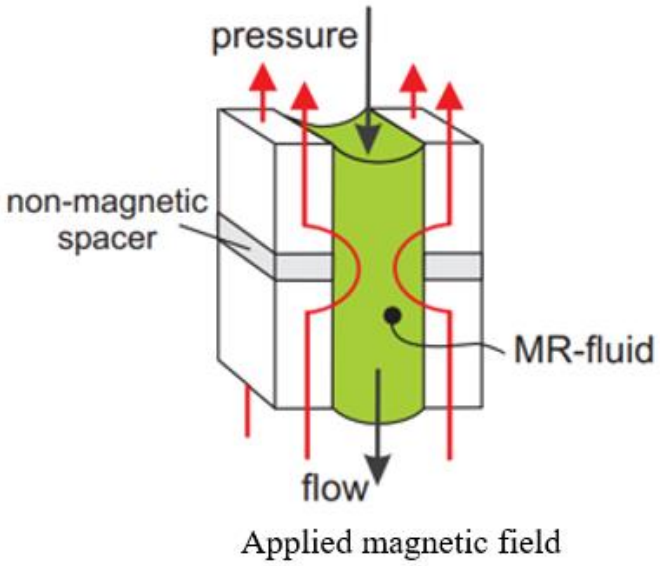

Figure 2.21 Pinch mode [74]

2.4.2. Magnetorheological devices with energy harvesting potential

The change in the rheological properties in the presence of a magnetic field makes MR fluids outstanding adoptions in vibration damping and mechanical shock attenuation in the area of engineering. Conventional dampers, also known as shock absorbers, absorb energy from a vibrating body and dissipate it in the environment. MR dampers, compared to traditional dampers, exploit the change in the rheological behavior of the fluid to vary their damping properties. MR fluids are liquids whose rheological properties are easily altered to cause torque transfer in vibration control devices. The stiffness of MR fluids may be altered to tune the vibration characteristics of mounts in suspension devices [71]. MR fluid devices are considered excellent dampers because of their long-range controllable damping force, fast response, and low energy consumption [76].

Magnetorheological dampers have been employed in many engineering applications such as the landing gears of airplanes to absorb the energy due to the impact and to reduce impact force transmitted to the airplane due to the impact on landing[78], high-speed train suspension system to enhance the comfort of passengers [79], seismic vibration reduction of engineering structures [11], gun recoil systems [80], washing machines [9] and many others. A current measurement system was designed using a piezo-laminated cantilever beam coupled with an electromagnetic coil-based MR fluid shearing setup [81]. The design and manufacture of a magnetorheological damper with internal pressure are also presented in [82]. A multifunctional MR damper consisting of a motor and MR fluid integrated into a single device and used as an actuator with multiple functions of motoring, clutching, and braking were designed [83]. Haiping et al. [84] carried out experimental studies of a semi-active MR damper subjected to repeated excitations and used a polynomial model to describe the dynamic response of the MR damper. A static output feedback H-infinity controller, which utilized the displacement and velocity of a spring-mass system as feedback signals for active vehicle suspension, was then designed.

Until recently, where much importance has been placed on designing autonomous systems with energy harvesting capability, the energy absorbed by MR dampers have always been wasted in the environment due to the unavailability of energy harvesting mechanism. Many researchers have proposed and designed MR dampers to harvest vibrational energy from the environment.

Currently, two different techniques and designs employing MR dampers with energy harvesting capability dampers have been proposed by several authors. One group of authors has proposed the transduction of linear motion in damper into rotary motion and use a

permanent rotational magnet DC or AC generators to harvest the kinetic energy. The other group has proposed the use of electromagnetic induction techniques to transduce the relative linear motion of permanent magnets and coils into electrical energy. The authors in [85] proposed MR fluid energy harvesting based on electromagnetic induction. The device consists of an array of magnets and inducing coils which convert the relative linear motion between the magnets and coil into energy. According to the authors, a rectified output voltage of 1.0 V was generated which is very low to power most magnetorheological fluid devices. A schematic of the proposed device is shown below:

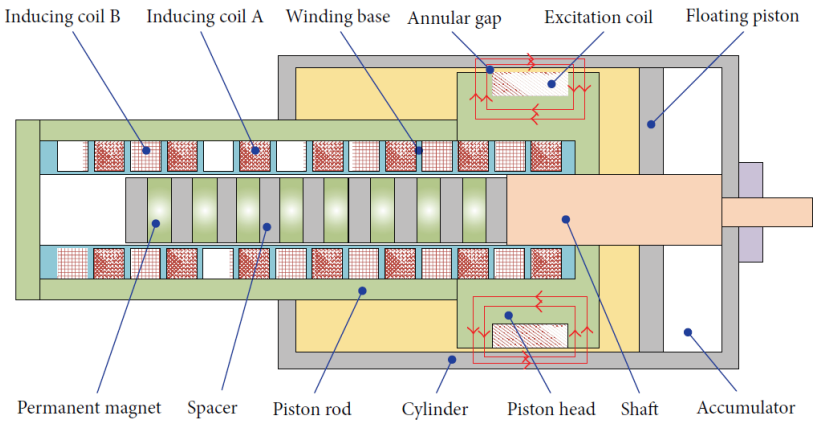

Figure 2.22 Schematic diagram of the MR damper with energy harvesting ability proposed by [85]

The design of a novel MR damper with self-powered capability is also presented in [86]. The proposed device is made up of a rotary energy harvesting unit with a permanent magnet DC generator as the energy generator. A ball screw mechanism is used to convert the translational motion of the damper into rotary motion. The energy generating system is integrated with the MR damper unit to form a single device. Figure 2.23 shows a schematic of the device.

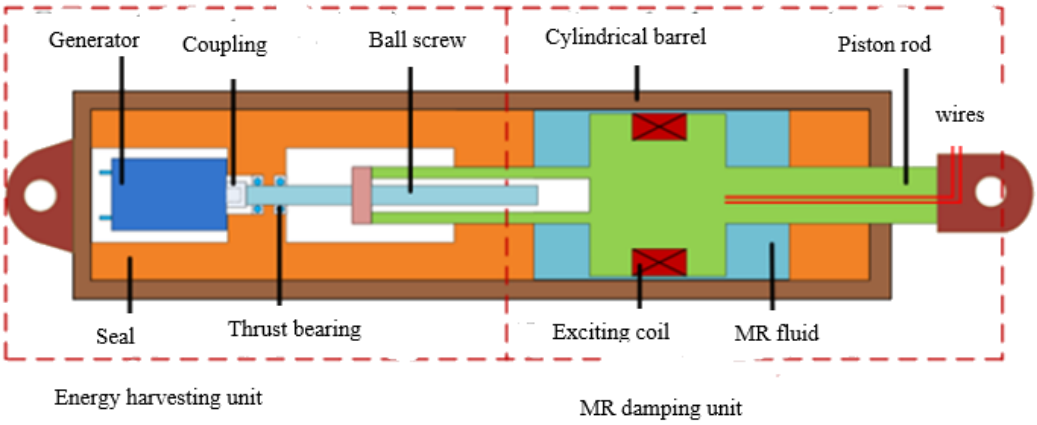

Figure 2.23 Self-powered rotary MR damper [86]

A linear energy harvesting MR damper to convert the waste energy from external vibrations, consisting of a damping unit and a power generation unit that converted the relative movement of the damper piston and the cylinder assembly into electrical power, was presented [87]. The energy harvesting damper integrates energy harvesting, dynamic sensor, and MR damping technologies into a single device.

Chen and Liao [88], proposed and investigated a self-sensing MR damper with power generation, which combines energy harvesting, sensing, and MR damping systems into one device. The MR damper had a power generation unit and velocity sensing capabilities and is it applicable to various systems. The device is a linear energy harvester and the fact it is an electromagnetic device makes it inefficient for small devices. A sectional view of the device is shown.

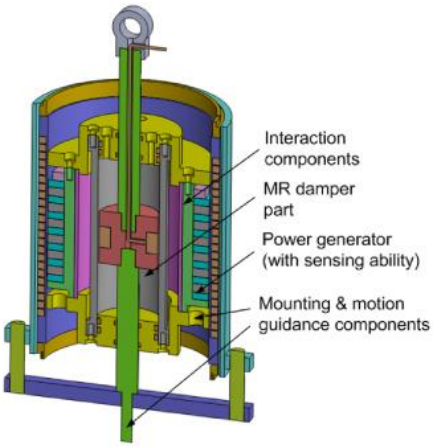

Figure 2.24 Sectional view of the self-sensing MR damper with power generation [88]

A power harvesting MR damper which combines a variable damping unit and the power generation system was proposed. The damping unit consists of an annular rotary gap filled with the MR fluids operating in pure shear mode. The rotary damping force was converted to a linear damping force using a ball-screw mechanism. The power generation mechanism is a permanent magnet AC generator, which converts the waste energy into useable electric energy to power the damping unit [89]. The energy converter reported by the authors is an electromagnetic generator which is widely known to be inefficient at the micro-level. Also, the use of the ball-screw mechanism further complicates the design.

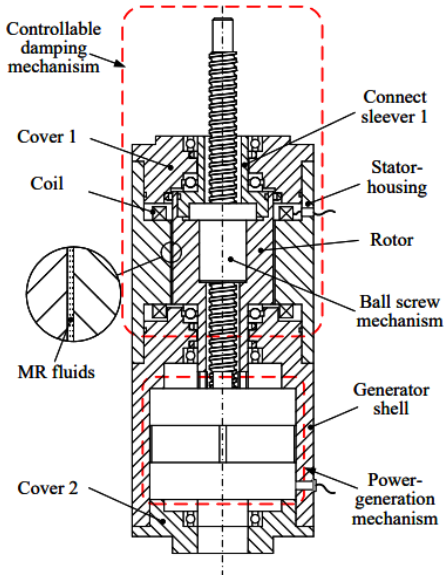

Figure 2.25 Structure of the power-generated magnetorheological damper [89]

Nakano et al. [90] proposed an active vibration control system that acted as a regenerative DC linear motor damper, which generated energy when the speed of the armature was high and stored it in a condenser. The energy stored was then used to activate the DC motor when the speed was low to drive an actuator in active vibration control. The system was able to achieve both regeneration and vibration control using a single DC motor. Tanner [91], also did some work on integrating shock and vibration control into a single isolation system by using an air spring connected in parallel with a controlled magnetorheological fluid damper. It was shown that the hybrid isolation system provides significantly improved performance over passive systems. These systems are not fully self-powered.

Furthermore, Sapinski et al. [92] investigated the positioning system-based using a rotary magnetorheological damper with power generation. Their system comprises an electromagnetic power generator, a magnetorheological damper that could change the damping properties of the system. An electrical circuit connected across the coil of the

generator and the damper control coil was then used to condition the voltage output from the generator. A sectional view of the damper is shown below:

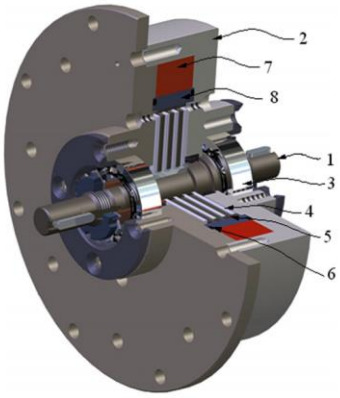

Figure 2.26 Cut-out geometry of damper: 1. Cylindrical rotor, 2. Ferromagnetic thin-walled cylinder, 3. Magnets, 4. Ball bearings, 5. Shaft, 6. Stator, 7. Rectangular frame, 8. Coil. [92]

Chen et al. [93] also proposed and implemented a self-power magnetorheological damper for motorcycle suspensions. In their system, a rack and pinion mechanism was used to convert the back and forth motion of the cylinder into a rotary motion. A DC motor was then used to convert the mechanical rotary motion into electrical power. The major drawback of this system is that, it is inefficient due to the conversion losses in the rack and pinion mechanism. The overall and internal structural views of the regenerative MR damper are shown:

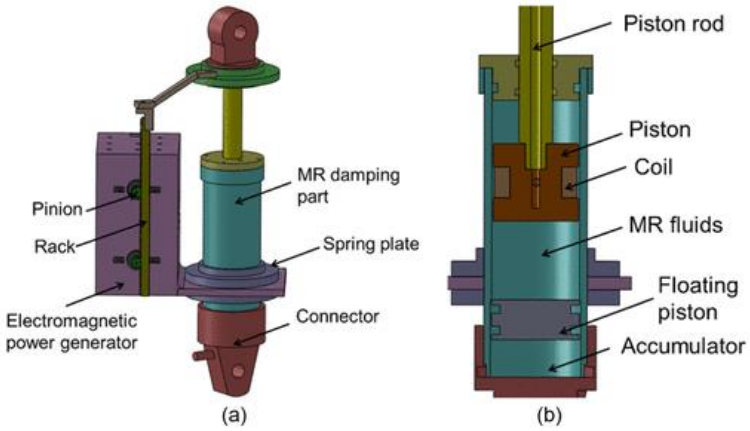

Figure 2.27 Structure of the proposed regenerative MR damper: (a) overall view; (b) internal structure of the MR damping part [93]

Raju et al. [94] also designed a magnetorheological damper based on its energy harvesting capability. In their work, a magnet and coil arrangement placed at the piston head of the damper was used as the energy-generating part of the damper. The authors reported 0.7 V and 0.45 V output voltages through COMSOL Multiphysics simulation and experimental study, respectively. The schematic of the system is shown.

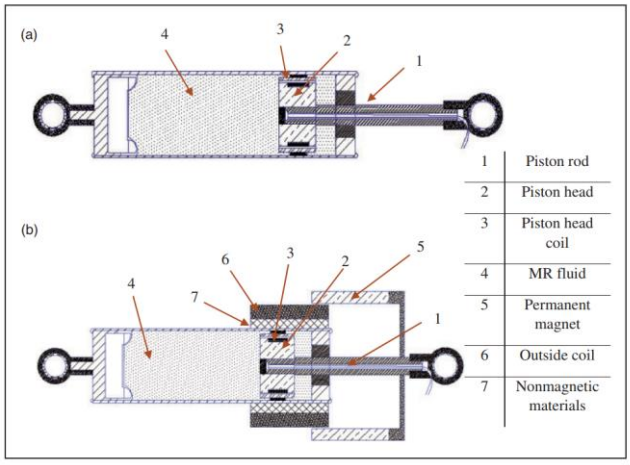

Figure 2.28 (a) Traditional magnetorheological damper and (b) proposed energy harvesting magnetorheological damper [94]

Additionally, a magnetorheological fluid seat suspension system with energy-generating ability was proposed by [95]. The seat suspension system consisted of a rotary magnetorheological damper and a permanent magnet DC generator. When the seat is excited by external vibration, the bases move to cause the scissor arms to rotate. The rotating motion of the scissor arms will cause the damping system to rotate. The rotary MR damper was used to provide the damping force. The rotary permanent magnet DC generator could provide the electrical power to dampen the vibrations and also transmit the signal based on the performance of the system to a control unit. The proposed scissor-like device is shown in Fig. 2.29.

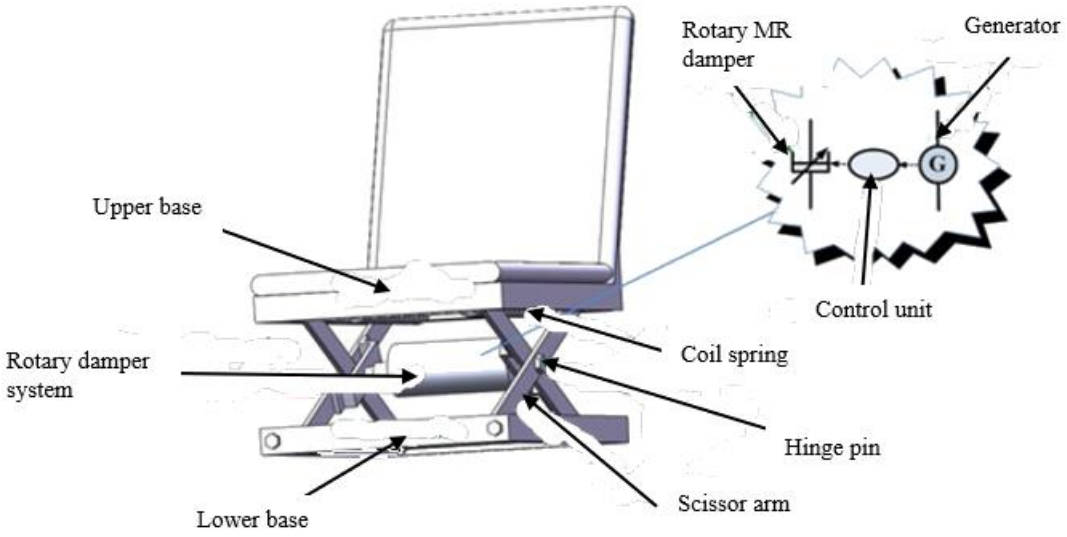

Figure 2.29 Ideal seat suspension with rotary MR damping system [95]

Another study in the field of self-powered MR devices was reported in [96]. The authors investigated a smart damping system consisting of a magnetorheological fluid damper and electromagnetic induction device in stayed-cable bridge vibrations control. The generator

unit of the proposed system uses a solenoid coil connected to the piston of the damper, which moves across stationary permanent magnets. The relative motion of the coil and the permanent magnet generates a voltage, which is used as an input to the MR damper to control its damping characteristics. The energy captured is used to power the damper which monitors the vibrations of the bridge.

Miao et al. [97] proposed an energy harvesting MR damper with a wireless sensing system to monitor the damper performance. The proposed energy harvesting device consists of an electromagnetic converter attached to an impeller. Maximum power of 28.1 mW at a frequency of 4 Hz was reported when a current of 0.5A was supplied to the damper.

Or et al. [98] developed a novel magnetorheological fluid damper embedded with pre-stressed piezoceramics to enable real-time vibration monitoring of mechanical and civil structures. The device is essentially the normal MR dampers but with the piezoelectric material and attached to the lower part of the damper to sense the vibrations. Thus, the device was designed mainly to sense the vibrations of structures not to harvest energy. It is, however, worth stating that the device could also be used to harvest the waste energy to activate the MR fluid and also power other accessories. This type of system is bulky and, therefore, not applicable with MEMS devices. The schematic of the device is shown below.

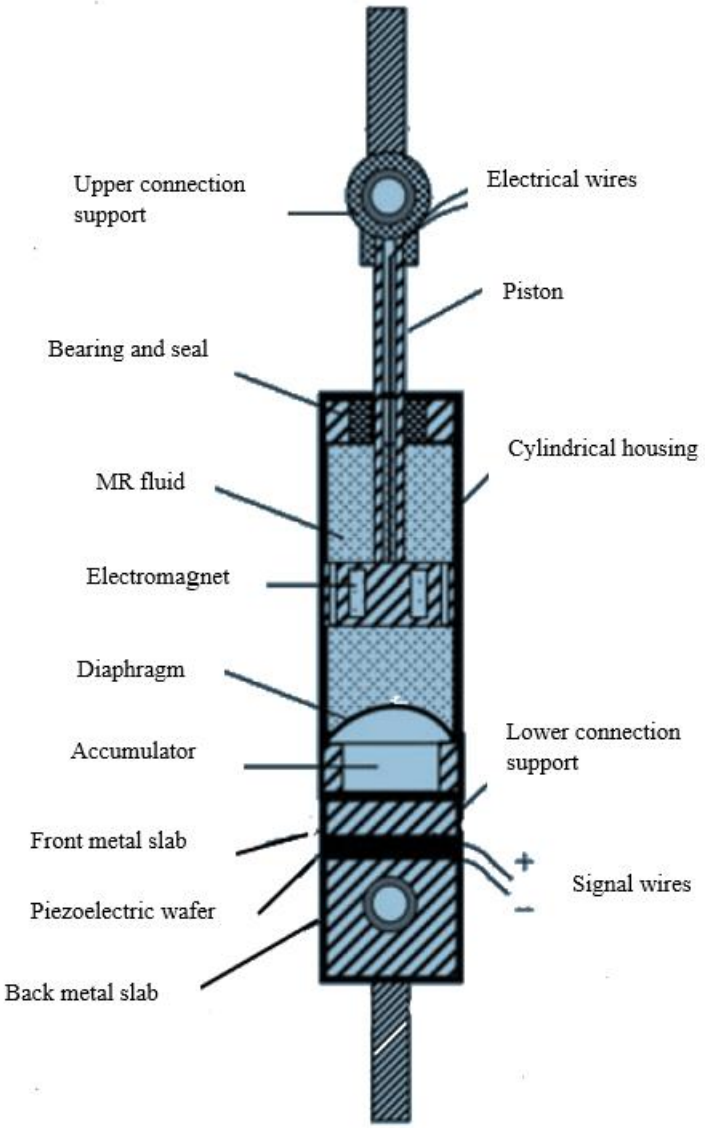

Figure 2.30 Schematic of MR damper with embedded pre-stressed piezoelectric material acting as a force sensor [98]

2.4.3. Various mathematical models used to describe the behavior of MR fluids

Models are an important part of the design and improvement of any engineering device. The success of MR fluids can be attributed to the extensive research which has been devoted to the development of accurate models to predict fluid behavior and consequently to develop high-performance MR devices. Bingham laid the foundation of MR and ER fluids modeling when he introduced his flow equation known as the Bingham flow equation [99]. Modeling of MR fluid behavior has since attracted much more consideration. Due to the complex and nonlinear nature of MR fluids, a multiplicity of models has been used to model their behavior. Some of the models are highlighted here.

In the absence of any magnetic field, MR fluids are considered Newtonian fluids whose shear stress (τ) is directly proportional to the shear rate ($\dot{\gamma}$). Newtonian fluid behavior is described by:

$$\tau = \eta\dot{\gamma} \tag{2.6}$$

η is a constant representing the viscosity of the fluid.

Upon the application of a magnetic field, the micron-sized particles align to form chain-like structures. These chain-like structures restrict the flow of the fluid, increasing the overall yield stress of the fluid. The behavior of the fluids is modeled as Bingham plastic with a variable field-dependent yield stress. The Bingham constitutive relation can be written as [99]:

$$\tau = \tau_y + \eta\dot{\gamma} \qquad |\tau| > |\tau_y| \tag{2.7}$$

τ_y is the field-dependent yield stress. At shear stresses smaller the yield stress, the fluid behaves as a viscoelastic material which is governed by:

$$\tau = G\dot{\gamma} \quad \tau < \tau_y \tag{2.8}$$

Where G is the material storage modulus. This storage modulus has also been found to be field-dependent [100].

The Bingham model has been used to design and characterize various MR fluid-based devices. That notwithstanding, real MR fluid behavior departs significantly from that simple model. One of these departures is the non-Newtonian behavior of the fluid, even in the absence of a magnetic field [101].

Furthermore, the Herschel-Bulkley model is another viscoelastic model that has been used to describe the behavior of MR fluids. This model takes into consideration the post-yield shear thinning or thickening behavior exhibited by MR fluids. The Herschel-Bulkley model is expressed as [102], [103]:

$$\tau = \tau_y + K|\dot{\gamma}|^{\frac{1}{z}} sgn(\dot{\gamma}) \qquad (2.9)$$

K and *z* are termed as the consistency parameter and flow behavior index, respectively. For $z>1$ the fluid exhibit thinning behavior, while the shear thickening fluids are described by $z<1$.

Another model which has been used to characterize the fluid behavior is the Bisvicous model. This model is constituted by static and dynamic yield stresses τ_1 and τ_2 respectively. When the shear stress is smaller than the static yield stress, the pre-yield behavior is assumed to be Newtonian with a pre-yield viscosity that is much larger than the post-yield viscosity [103]. The model is represented as [104]–[106]:

$$\tau = \begin{cases} \tau_y + \eta\dot{\gamma} & |\tau|>\tau_1 \\ \eta_r\dot{\gamma} & |\tau|<\tau_2 \end{cases} \qquad (2.10)$$

Where η_r is a constant representing the elastic properties of the fluid.

Figure 2.31 shows the Bingham plastic, and Herschel-Bulkley models whiles Figure 2.32 portrays the Bisviscous model.

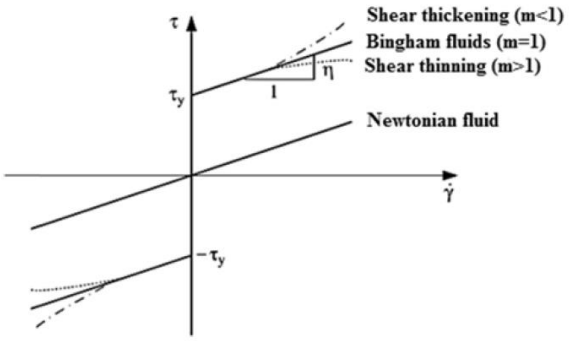

Figure 2.31 Bingham model and Herschel-Bulkley model [99]

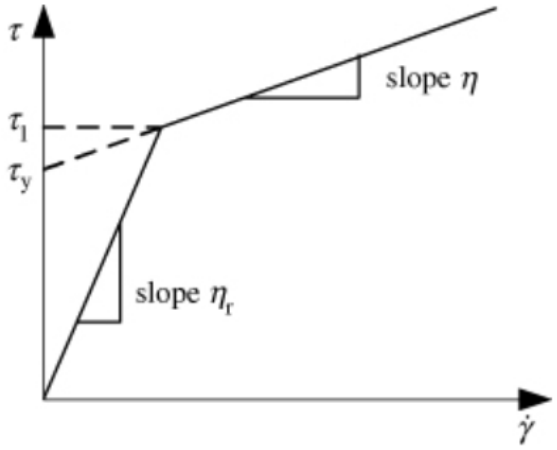

Figure 2.32 Idealised biviscous model [104]

The Bingham model has been employed in several studies to characterize the behavior of specific MR fluid devices. Most of such works are based on the work of [107], who addressed Bingham flow in channels with parallel walls and introduced non-dimensional forms of the Bingham model. Gavin et al. [108]utilized the approach proposed by Phillips to develop a model for ER fluid flow in an ER damper using the parallel plate nondimensionalized numerical approximation. They solved the Navier-Stokes equations for a steady flow of an electrorheological fluid through annular ducts. Based on their

analyses, they were able to predict that the dynamic force range of dampers increases exponentially with the ratio of the gap size to plunger diameter.

Stanway et al. [109] put forward an idealized model based on the Bingham model to describe the performance of MR dampers. They used a viscous damper in parallel with a Coulomb friction element to denote the force produced by the damper. The force is described by:

$$F = f_c sgn(\dot{x}) + c_0 \dot{x} + f_0 \tag{2.11}$$

Where $\dot{x}$ is the piston velocity, c_0 is viscous damping coefficient, f_c is the frictional force and f_0 is an offset force to account for the presence of an accumulator.

In a similar work, Wereley and Pang [110] used parallel plate approximation based on a non-dimensional analysis of ER and MR fluid dampers. The authors introduced another set of non-dimensional numbers, which are the same as those used by Hu and Wereley [111] to perform a non-dimensional damping analysis of flow-mode MR and ER dampers.

Kamath et al. [112] and Gavin et al. [113] developed quasi-steady axisymmetric models of ER fluid dampers. Also, Yang et al. [114] developed a similar model for large-scale MR fluid damper.

To account for the shear-thinning/thickening effect, the Herschel-Bulkley model, in which the post-yield plastic viscosity is dependent on the shear strain rate, is also used in other studies. Wang and Gordaninejad [115] used the Herschel-Bulkley model to develop models for ER and MR fluid flowing in pipes and parallel plates. A uniform and one-dimensional laminar flow was assumed in the model derivation. Also, they used dimensionless variables were used to represent the continuity and momentum equations. The non-dimensional plug thickness was determined to be an important variable in developing basic expressions for

the analytical solution. Also, Lee and Wereley [116] and Wang and Gordaninejad [117] proposed a model for an ER/MR flow mode damper which employed the Herschel-Bulkley constitutive model. In a thorough study by Yang [118], the author developed axisymmetric models of a large-scale MR fluid damper from the Herschel-Bulkley model and the Bingham model. He compared the axisymmetric models to models developed using the parallel plate approximation and showed that the maximum error in the predicted force is less than 2%.

Apart from the Bingham plastic, Herschel-Bulkley and Bivicous models (generally known as parametric models), other models termed as nonparametric models have been used to describe the dynamic behavior of MR fluid devices. Nonparametric models make use of polynomial approximation or black-box modeling techniques [119]. Examples of such nonparametric models include neural networks, fuzzy modeling, etc.

Neural networks have been employed to characterize complex engineering systems. They are generally trained to learn how a set of inputs and outputs relate to each other. This immense capability has been employed to model MR dampers. An alternative representation of MR damper using a multilayer perceptron neural network (MLP) has been proposed by [120]. They used a neural network model with 6 input neurons, one output neuron, and twelve neurons in the hidden layer to simulate the dynamic characteristics of the MR damper. The model was trained using Gauss-Newton based Levenberg-Marquardt method using data obtained from the simulation of the differential equations. An optimal brain surgeon technique was then used to trim the weights and to improve the neural networks. An optimal neural network was then used to model the dynamic behavior of the MR damper.

Also, Wang and Liao [121] used a direct trained identification neural network to model and to predict the damping force of a magnetorheological fluid damper on line based on dynamic responses across the damper and the command voltage. Cao et al. [122] used a grey-box hybrid approach that combines the physical principles and neural networks to better predict the MR damper dynamics. Boada et al. [123] used a recursive lazy learning method based on neural networks to model MR damper behavior.

The fuzzy logic technique has also been used to model MR damper characteristics. A forward fuzzy model that portrays non-linear behavior, such as hysteretic and field-dependent behavior, and which produced a force for given operating conditions and control voltage, was devised and described in [124]. Based on the concept of a mathematical involution, inverse fuzzy models for control analysis were derived from the proposed forward fuzzy model. Xiufang and Shumei [124] proposed a hybrid modeling strategy using a shuffled frog-leaping algorithm and adaptive network-based fuzzy inference system to describe the inverse dynamic characteristics of MR dampers. A combination of fuzzy logic and neural network is presented in [125]–[128] to improve the adaptability of the proposed systems.

Polynomial models have also been used to model the dynamic characteristics of MR fluid devices. Choi et al. [129] used a sixth-order polynomial model based on trial and error to model the hysteresis characteristics of MR damper. Leva and Piroddi [130], used a linear-in-the-parameters polynomial NARX model to identify the MR damper model parameters without requiring a priori structural information. Song et al. [131] used a nonparametric model to accurately predict the damping force dynamics, damper bilinear behavior, hysteresis, and electromagnetic saturation using a series of numerical mathematical

functions. Also, Yun and Masfi [132] used a nonparametric system identification approach based on a two-dimensional series expansion of the Chebyshev polynomials to model an MR damper. Kim et al. [133] proposed a describing function method to model the nonlinear dynamics of squeeze film dampers.

Mori and Sano used a query-based modeling technique [134], and a look-up table method [135] are other modeling techniques that have been used to describe MR dampers based on the storage of input-output dataset.

2.5. Gaps in the Literature

Magnetorheological fluids are mainly used in vibration control systems. It is, therefore, not surprising the literature reported is mainly focused on its usage in vibration damping devices. The literature on MR fluid devices with energy harvesting capabilities is comprehensive. These mainly used electromagnetic devices with mechanical motion converters such as rack and pinion to harness the waste energy available in vibration suppression systems to power the dampers. Electromagnetic energy conversion is a well-established technique, but it is very inefficient at the micro-scale level. It requires a large number of turns of conductors to generate enough voltage to power sensors. It is currently very difficult to design a micro-electromagnetic transducer with a large number of turns using the well-known thin deposition and micro-fabrication techniques. The direct use of the fluid rheological properties to advance in the energy harvesting techniques is not much reported. There is currently a major gap in the application of MR fluids in piezoelectric energy harvesting. Piezoelectric energy harvesters suffer greatly when there is a slight shift in the source frequency. This requires frequency matching and the variable stiffness of MR

fluids makes them a potential solution to the frequency matching problem. It is worth mentioning that, apart from the work started by our research group, no literature is available on the application of MR fluids in piezoelectric energy harvesting.

Chapter 3: Theory and Methodology

The section provides a detailed description of the proposed energy harvesting technique, the theoretical background for the analysis. In addition, it describes the experimental setup and procedure.

3.1. Description of Proposed Energy Harvesting Technique

The energy harvesting system is depicted schematically in Fig. 3.1. The system consists of a piezoelectric bimorph device placed between two magnets and a layer of fluid placed on top of one of the magnets. The bimorph actuator used here is the M1100 from Johnson Matthey Piezo-Products [136]. This piezoelectric bimorph is made up of a shim layer of copper (depicted in the orange color in Fig. 3.2), PZT (shown in black in Fig. 3.1), and gold-coated ends acting as the electrodes. Note that, the orange end of Fig. 3.2 is not visible in Fig. 3.1 because it is clamped.

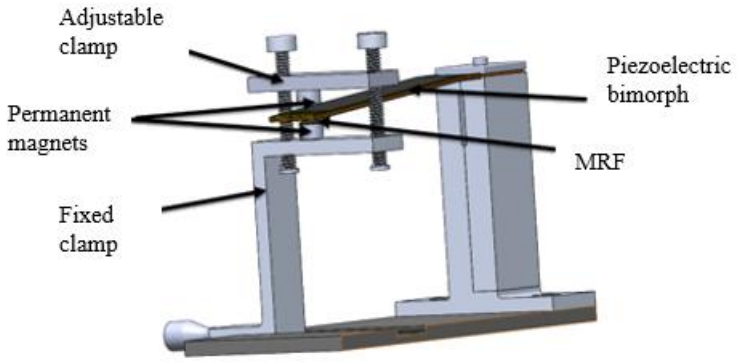

Figure 3.1 Schematic of the soft-impact energy harvester [137]

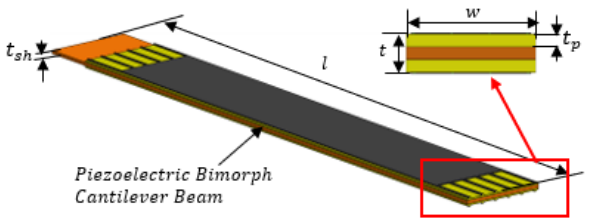

Figure 3.2 Piezoelectric bimorph bending actuator

3.2. Theoretical Model

The impact energy harvester studied here thesis is modeled as a piecewise coupled nonlinear single degree of freedom (SDOF) system [56], [138]. The model used here is considered piecewise because it is defined under a sequence of intervals depending on whether there is impact or not. Also, the nonlinearity of the model is due to the fluid which is nonlinear. The model consists of a mechanical part and electrical part coupled together through the electromechanical coupling coefficient. In this model, when the beam displaces more than the initial gap, it impacts the MR fluid, and the vibration characteristics of the beam change from linear to nonlinear due to the nonlinear force added to the beam due to the impact [137]. The spring constant and damping coefficient of the piezoelectric beam change from k_1 to $k_1 + k_2$ and c_1 to $c_1 + c_2$ respectively. The SDOF model is depicted schematically in Fig. 3.3.

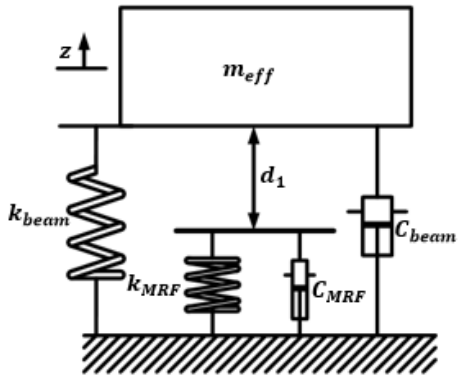

Figure 3.3 Schematic of the model of the energy harvester [67]

The dynamic equations which describe the behavior of the system are piecewise nonlinear. The Heaviside function (also commonly referred to as a step function) is a discontinuous function and is used mostly to model a signal that is off at a certain time and on indefinitely. The Heaviside function, therefore, is used to model the piecewise nonlinear and inelastic dynamics of the system as it accurately describes the dynamics of the system at the different states (thus, when there is impact and no impact). These equations are represented as:

$$m\ddot{x} + c_1\dot{x} + k_1x + (c_2\dot{x} + k_2x)h = Fsin(\omega t) - 2\theta v \tag{3.1}$$

$$-\theta\dot{x} + C_p\dot{v} = -\frac{v}{2R} \tag{3.2}$$

where, m, is the mass of the cantilever beam, c_1 represents the damping coefficient of the beam, c_2 represents the damping coefficient due to the MR fluid. The stiffness of the beam alone is denoted by k_1 and when the beam impacts the fluid, the stiffness k_2 is added to it. *x* is the displacement of the cantilever beam. The output voltage of the energy harvester is represented by *v*. R, θ and C_p are the load resistance, piezoelectric coefficient (forcing factor), and the piezoelectric plate capacitance, respectively. h is the Heaviside function and is defined by the piecewise relation:

$$h = \begin{cases} 0, & x < d_1 \\ 1, & x \geq d_1 \end{cases}$$

where d_1 is defined in Fig. 3.3.

The equation is based on the parallel connection of the piezoelectric bimorph layers. The forcing factor for the bimorph configuration is defined as [139]:

$$K_e{}^2 = \frac{2\,\theta^2}{C_p k} \tag{3.3}$$

where K_e is the piezoelectric coupling coefficient and k is defined as the effective stiffness of the beam.

The main parameter of the MR fluid is the magnetic field-induced yield stress. In this thesis, MR 140-CG, from Lord Corporation was used for the study [140]. The characteristics of the fluid are described by two empirical equations [141]. Equation (3.4) represents yield stress, $\tau(H)$, as a function of the field intensity H , while Equation (3.5) defines the B/H curve of the fluid.

$$\tau(H) = 271700 \times \mathrm{C} \times \Phi^{1.5239} \times \tanh(6.3310^{-6} \times H) \tag{3.4}$$

$$B = 1.91{\times}\Phi^{1.133} \times (1 - e^{-10.97\mu_o H}) + \mu_o H \tag{3.5}$$

Where C is a constant whose value depends on the type of carrier fluid of the MR fluid and Φ is the particle volume fraction of the fluid.

A graph of the yield stress vs magnetic field for the fluid is shown in Fig. 3.4.

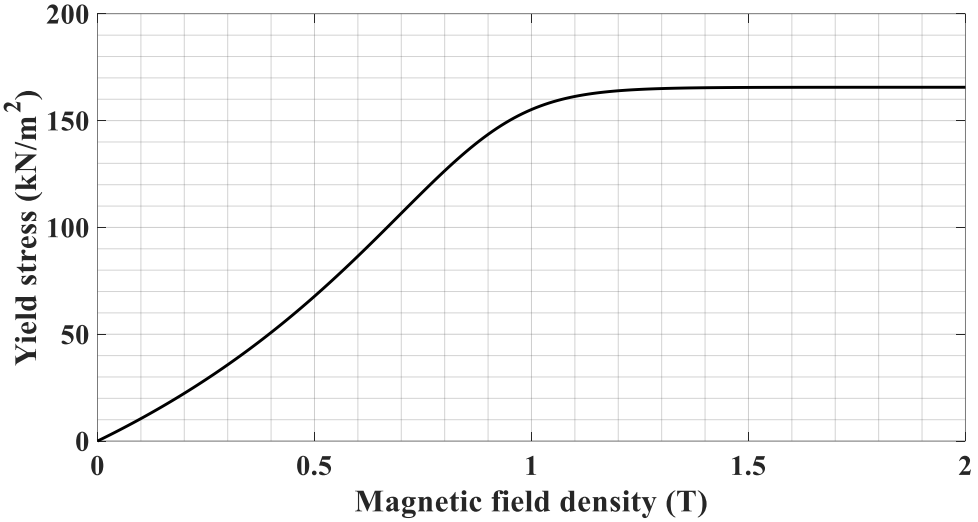

Figure 3.4 Magnetic field vs yield stress of MR 140-CG

The stiffness and damping due to the fluid depend on the generated force due to the impact. The total force generated is given by [142], [143]:

$$F_{MRF} = \frac{4\pi r^3 \tau}{3(d_1+x)}\, sgn(\dot{x}) + \frac{3}{2}\frac{\pi \eta r^4}{(d_1+x)^3}\dot{x} \tag{3.6}$$

where r denotes the radius of the magnet, and η is the plastic viscosity of the fluid. The force generated has two components: spring constant component which is controlled mainly by the yield stress, and the passive force which yields the damping coefficient. By taking the derivative of the spring force with respect to x, the stiffness due to the fluid is obtained as:

$$k_2 = \frac{4\pi r^3 \tau}{3(d_1+x)^2} \tag{3.7}$$

The damping coefficient of the fluid is obtained as:

$$c_2 = \frac{3}{2}\frac{\pi \eta r^4}{(d_1+x)^3} \tag{3.8}$$

The model used to describe the squeezing effect of the fluid has been experimentally validated by [72].

The stiffness of the piezoelectric beam alone is defined as [5]:

$$k_1 = \frac{3EI}{{l_b}^3} \tag{3.8}$$

where E is Young's modulus of the piezoelectric beam, I is the moment of inertia of the beam and l_b is the free vibrating length. The moment of inertia is given by [144]:

$$I = \frac{w}{12}\left(\frac{E_{sh}}{E_p}{t_{sh}}^3 + 2{t_p}^3\right) + \frac{wt_p}{2}(t_{sh} + t_p)^2 \tag{3.10}$$

where *w* represents the width of the beam, E_{sh} denotes the modulus of elasticity of the shim layer, E_p is Young's modulus of the piezo-ceramic material, t_{sh} is the thickness of the copper layer (middle layer or shim), and t_p is the thickness of piezo-ceramic material.

The frequency of the energy harvester is, therefore, determined using the parameters defined above and it is given as:

$$\omega_n = \sqrt{\frac{K_{eff}}{m}} \tag{3.11}$$

K_{eff} is defined as the overall stiffness of the beam and it is equal to the sum of k_1 and k_2, and m is the mass of the energy harvester.

Energy from vibration is mostly harvested through damping. The damping ratio of the system is a quantity used to denote energy dissipation. The damping coefficient of the piezoelectric cantilever beam alone is defined by Equation (3.12) [145]:

$$c_1 = 2\zeta m\omega_{beam} \tag{3.12}$$

ζ is the damping ratio of the free vibration beam.

The simulation is performed assuming a harmonic excitation with an acceleration amplitude of 1g, (where $g = 9.81\ ms^{-2}$). It is worth stating that this value was chosen arbitrarily, however, it is within typical vibration levels of most sources available in the environment [5]. The parameters of the piezoelectric bimorph and the fluid are listed in Table 3.1 below.

Table 3.1 Parameters of the proposed energy harvesting system

Symbol	Description	Value	Unit
l_b	Free (vibrating) length of beam	39.5	mm
w	Width of beam	7.2	mm
t_p	Piezoelectric layer thickness	0.25	mm
t_{sh}	Shim layer thickness	0.28	mm
ρ_p	Piezoelectric layer density	8100	Kg/m^3
ρ_{sh}	Shim layer density	8960	Kg/m^3
E_{sh}	Shim layer modulus of elasticity	120e9	N/m^2
E_p	Piezoelectric layer modulus of elasticity	8.55e11	N/m^2
r	Radius of magnet	2	mm
h_m	Hight of magnet	6	mm
p_m	Density of magnetic	7500	Kg/m^3
Φ	Particle volume fraction	0.4	
$\boldsymbol{\eta}$	Viscosity of MR fluid	0.3	Pa.s
R	Load resistance	200	kΩ
μ_0	Permeability of free space	1.26e-6	H/m
d_1	Initial gap between MRF and Beam	0.5	mm
C	Coefficient dependent on the carrier fluid of MRF	1	
$\boldsymbol{K_e}$	Piezoelectric coupling coefficient	0.42	

3.3. Experimental Setup

The set up used to validate the numerical results is displayed in Figure 3.5. This consists of the piezoelectric cantilever beam (M1100), two Nd-Fe-B (N30) magnets, a signal amplifier with a built-in sinusoidal wave generator (model LA-100 signal amplifier), Sentek MS-50 vibration shaker with a maximum acceleration of 100 g and a frequency range of 5-2500 Hz, Keyence laser displacement sensor (IL series) with measurement range of 20 mm to 45 mm and linearity of $+0.1\%$ of full-scale reading, an electromagnetic gaussmeter (Allosun EM556) with a measurement range of 0.1 to 199.9 mG (milligauss), 333B50 accelerometer from Piezotronics (with a sensitivity of 1000 mV/g) and an oscilloscope (RTB2014). The cantilever beam (bimorph) is then mounted on the vibration shaker and placed between the two magnets. The magnets are attached to an adjustable clamp to enable variation of the distance between them and hence the magnetic field. The fluid (about 0.5mm) is then attached to the bottom magnet.

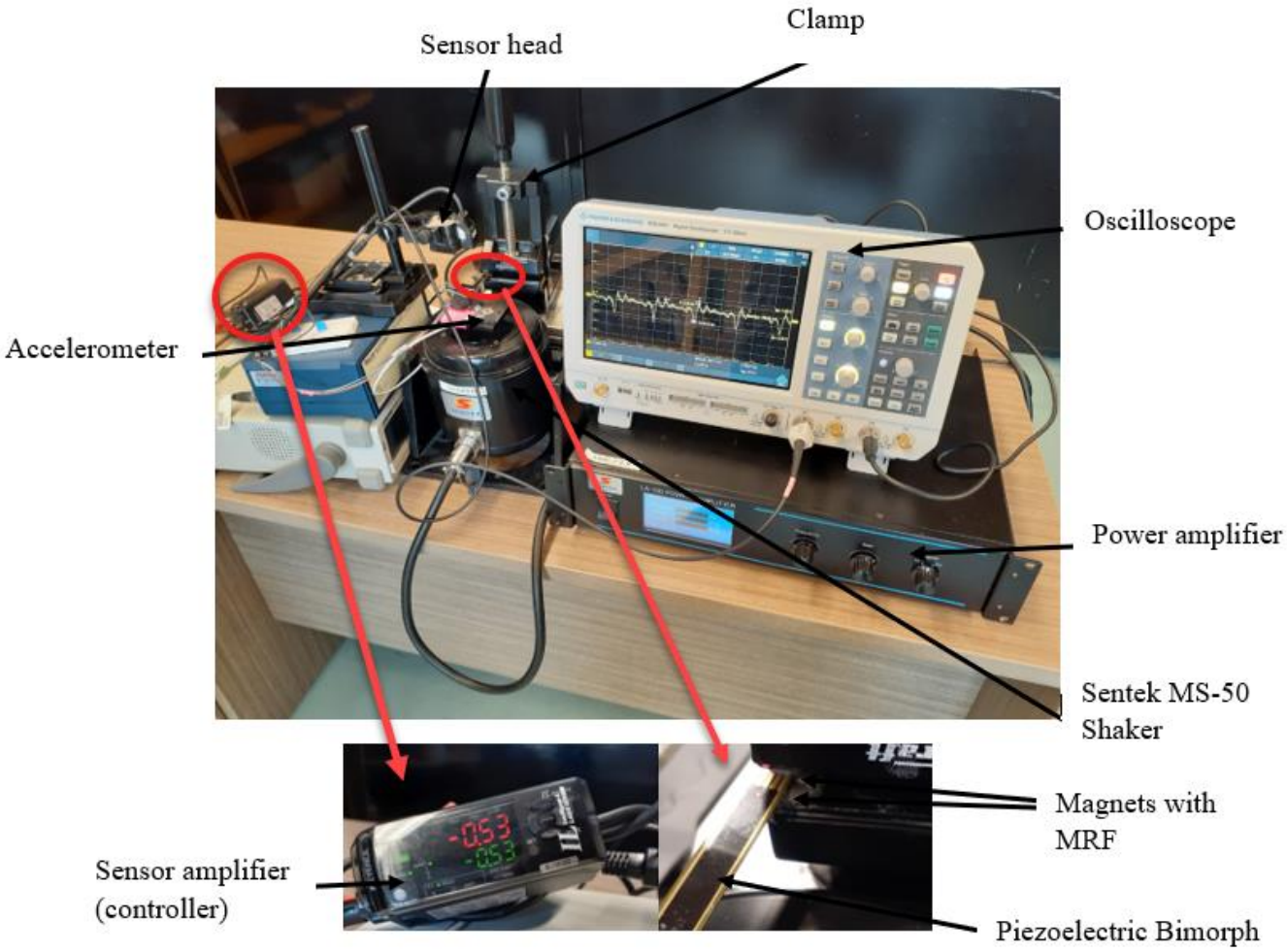

Figure 3.5 Experimental setup

3.4. Experimental and Numerical Test Conditions

The test conditions considered for the study are mainly a variation of the distance between the magnets to apply different magnetic fields to the fluid, the size of magnets, and how the load resistance affects the generated voltage of the piezoelectric energy harvesting device. With regards to the distance between the magnets, 2.8 mm, 5 mm, and 7 mm distances were considered and these correspond to magnetic fields of 0.13 T, 0.085 T, and 0.044 T respectively. The generated voltage depends on the load resistance connected

across the terminals of the piezoelectric bimorph. The load resistance is varied from 10 kΩ to 200 kΩ. The size of the magnet also affects the performance of the system as the total squeeze force depends on it. In this thesis, the size of the magnet is varied from 0 (no fluid condition) to 7 mm radius. These conditions are reported in the table below:

Table 3.2 Test conditions

Parameter	Value	Measured quantity value (T)
Distance between magnets (mm)	2.8 mm	0.13
	5.0 mm	0.085
	7.0 mm	0.044
Radius of magnets (mm)	0 to 7 mm	
Load resistance (kΩ)	10 to 500	

3.5. Experimental Procedure

In this work, a sinusoidal signal of 1g constant amplitude (shown in Fig. 3.6) is applied to the piezoelectric cantilever beam via the vibration shaker (Sentek MS-50). The vibration is monitored by the accelerometer. This signal was obtained by driving the shaker with a sine wave of 20 Hz at 1.7 volts and 0.2 Amps from the amplifier to obtain the magnitude of 1g acceleration (9.81 ms^{-2}). The displacement sensor, which consists of a sensor head (IL-030) and an amplifier control unit (IL-1000), is used to monitor the displacement of the cantilever beam. A frequency sweep from 15 Hz to 150 Hz is carried out to determine the frequency response of the energy harvester. A resistive load of 200 kΩ is connected across the bimorph terminals, which in turn is connected to the digital oscilloscope to

monitor and record the generated voltage in time. The results are then analyzed in MATLAB.

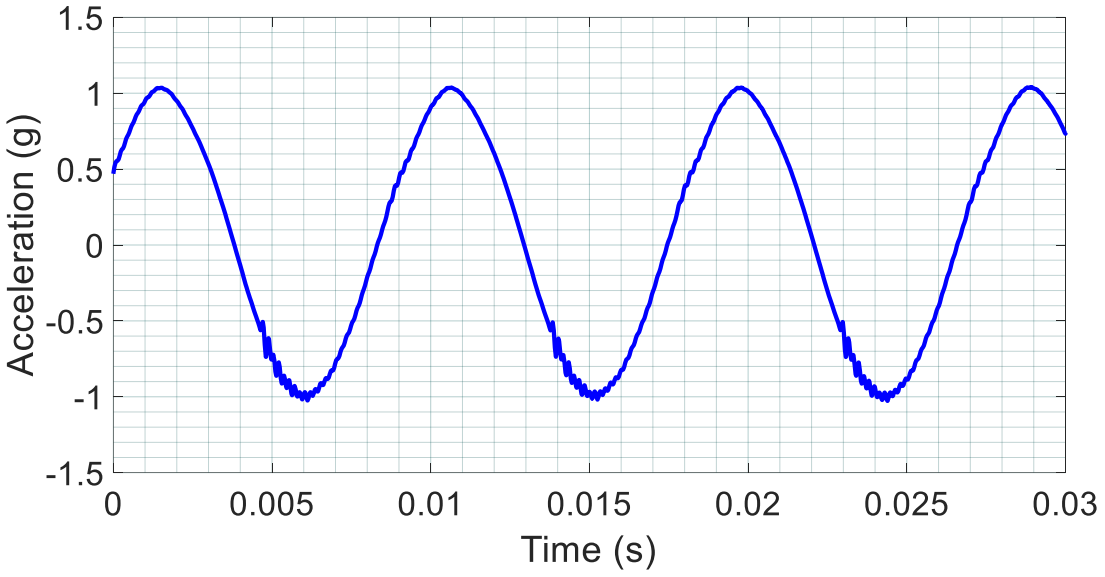

Figure 3.6 Excitation signal applied to the piezoelectric bimorph beam

3.6. Error Estimation

To better understand and to investigate the system performance effectively, each component of the system was carefully examined to ensure they performed within a certain margin of error. To ensure that the piezoelectric cantilever beam was excited at the right acceleration level, the accelerometer (with an accuracy of ± 2 % and a reference sensitivity of 1000 mV/g) was self-calibrated with a low frequency portable mini shaker (394C06 handheld shaker from Piezotronics). This shaker is specifically designed to verify accelerometers performance by driving them with a constant sine wave of 159.2 Hz frequency and 9.81 ms^{-2} acceleration. The calibration gave the sensitivity of the acceleration to be $1018\, mV/g$ which represents a deviation of about 2% from the

manufacturer's value of $1000\ mV/g$. The oscilloscope is another instrument that always requires calibration to compensate for signal attenuations in the probes. The oscilloscope used in this thesis is the ROHDE & SCHWARZ RTB 2014 digital oscilloscope with a minimum sensitivity of $1mV/division$ and accuracy of 1.5 %. To determine the total uncertainty of the oscilloscope, ten tests were performed to obtain a reference voltage. Also, the average and standard deviation of the test values were determined. In addition, the probes were adequately compensated by connecting the terminals to the connectors of the oscilloscope. Since voltage recorded by the oscilloscope was far greater than the sensitivity of a millivolt per division, it is fair to conclude that the error introduced by the oscilloscope was very minimal. Also, the Gaussmeter has an accuracy of $\pm 10\ \% + 8$ digits.

With regards to the piezoelectric bimorph, the parameter that could be verified was the free vibrating length. A free vibrating length of 38 mm was used as the electrode coating covers that much length. The length quoted by the manufacturer is $49.95\ \pm 0.05$ mm for the whole cantilever and the ceramic covers only 45 ± 0.01 mm. Thus, choosing a free length vibrating of 38 mm was therefore reasonable. The piezoelectric constants could not be verified since there was no means to do so. The piezoelectric constant that was necessary in this work was the coupling coefficient and this is quoted as 0.42 (from the manufacturer's datasheet) for 31-mode adopted in this thesis work. This constant essentially provides an idea of how much of the mechanical input energy is converted to electrical energy.

Based on the equipment accuracies and reference values chosen for each equipment, the total uncertainty associated with each equipment was computed and reported in Table 3.2.

As shown in the table, the most significant error is from the electromagnetic Gaussmeter. Thus, the major discrepancies between the numerical and experimental results are due mainly to the measurement of the magnetic field.

In conclusion, the components that could introduce significant error and could easily be verified through calibration are the accelerometer and the oscilloscope, and these were duly calibrated.

Table 3.3 Uncertainty of the system components

Device	Quantity measured	Reference value (C_1)	Absolute uncertainty (C_2)	Relative uncertainty (C_3)	Relative precision error (C_4)	Total uncertainty (C_5)
Oscilloscope	Voltage	5 V	0.075	0.015	0.052	0.054
Accelerometer	Acceleration	1000 mV/g	20.000	0.020	0.041	0.046
Gaussmeter	Magnetic field	1.28 T	0.05	0.039	0.151	0.120

The following equations were used to calculate the various uncertainties in Table 3.2:

$$C_2 = accuracy \times C_1 \tag{3.1}$$

$$C_2 = \frac{C_2}{C_1} \tag{3.2}$$

$$C_2 = \frac{std}{ave} \tag{3.3}$$

$$C_5 = \sqrt{{C_3}^2 + {C_4}^2} \tag{3.4}$$

Chapter 4: Results and Discussion

In this section, the results obtained based on the test conditions are presented. The equations characterizing the energy harvesting system were solved using MATLAB differential equation solver. As mentioned in Chapter 3, the simulation was done under an excitation amplitude of $1g$ at a frequency of 20 Hz. The numerical study was performed at 0.04 T, 0.08 T, and 0.12 T magnetic fields. These magnetic field densities correspond to yield stresses of 1668, 3415 and 5265 N/m^2, respectively. These yield stress values were directly used in the simulation. The chapter is divided into five sections as discussed below.

4.1. Comparison of Voltage Output and Frequency for both Theoretical and Experimental

The peak-peak voltage versus time is represented in Fig. 4.2 for the numerical study. The piezoelectric beam used here was excited at a frequency lower than its resonant frequency. This is because, at high frequency, the beam vibrates with low displacement and high speed to obtain almost no impact. To able to vary the magnetic field, the experiment was carried out at various distances between the magnets. With the distance between the magnets set at 2.8 mm, a magnetic field of 0.13 T was measured, at 5 mm the field measured was 0.085 T and at 7 mm, 0.44 T was recorded by the Gaussmeter. Changing the distance between the magnets varies the magnetic field and solidifies (increases viscosity) the fluid to a different extent.

Figure 4.1 and Figure 4.2 represent the results of the voltage generated versus time for both the simulation and experimental studies, respectively. The results are also summarized in

Table 4.1. The differences in the profiles of the experimental and simulation results are due to the nonlinear characteristics of the fluid making it difficult to accurately model. The results obtained show that increasing the magnetic field increases the generated voltage from 9.29 V at the magnetic field of 0.04T to 9.42 V at 0.08T which is about a 1.4% increase for the simulation. With the experimental studies, the voltage increased from 7.71 V at 0.44 T to 8.46 V at 0.085T which is 9.7% increase. This increase is because of an overall reduction in damping ratio at high frequencies for any given system parameters [146]. As a general requirement in vibration energy harvesting, the mechanical damping should be kept low as much as possible. Furthermore, the frequency increased from the excitation value of 20 Hz to 59.58 Hz for the simulation and 61.02 Hz for experimental study when the magnetic field was set to 0.04 T. This is because the stiffness of the beam is increased from k_1 to $k_1 + k_2$ when it impacts the fluid. The oscillations in the voltage with the different amplitudes can be attributed to the 'stick' and 'release' effects of the fluid when the beam impacts it. Table 4.1 also shows a summary of the result of the frequencies at the different magnetic fields.

Table 4.1 Summary of experimental and simulation results

Magnetic field (Tesla)	Voltage (V)			Frequency (Hz)		
	Numerical simulation	Experimental	Difference (%)	Numerical simulation	Experimental	Difference (%)
0.04	9.29	7.71	17.01	59.58	61.02	2.4
0.08	9.42	8.46	10.2	82.76	83.03	0.3
0.12	9.53	9.06	5.00	101.70	103.00	1.3

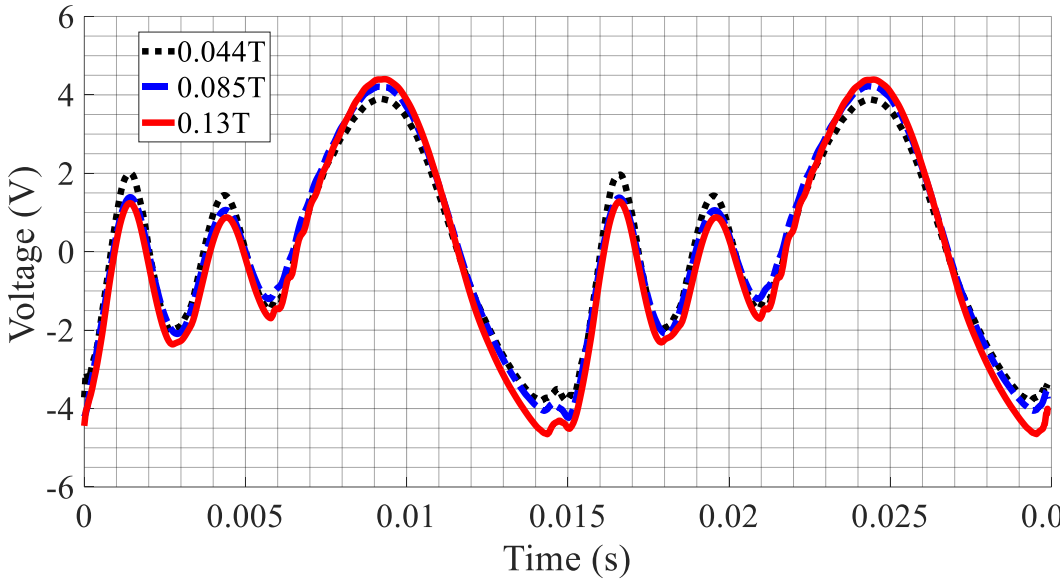

Figure 4.1 Voltage vs time for the selected magnetic field densities for a load resistance of 200 kΩ: Experimental study

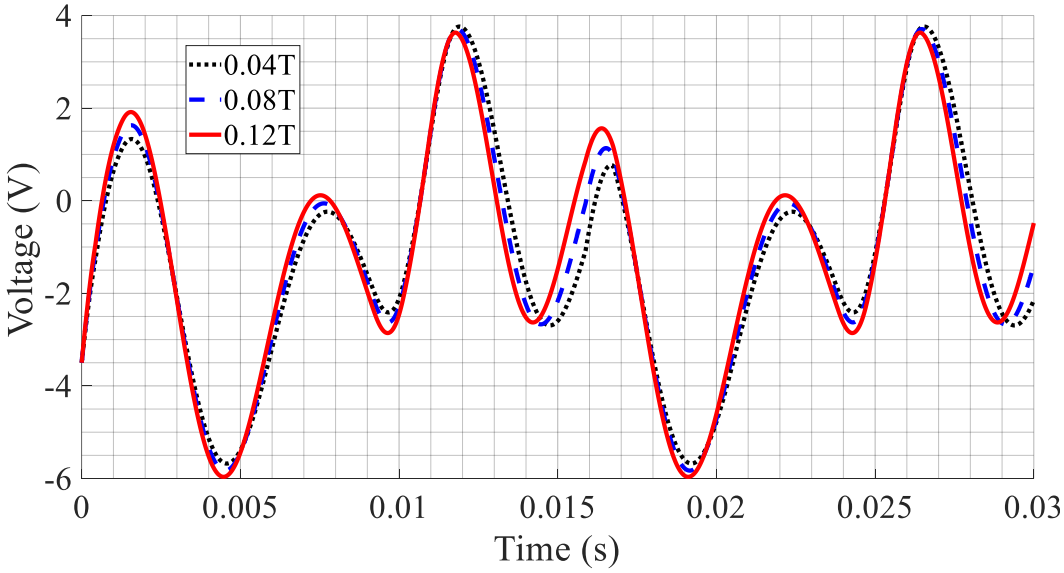

Figure 4.2 Numerical results of the voltage generated for the different magnetic field densities for a load resistance of 200 kΩ

Figure 4.3 shows the voltage and power results for the energy harvesting system at different load resistances. The power is maximum at a certain load resistance, termed as the optimum

resistance. The optimum load is the load resistance that is equal to the resistance of the piezoelectric plates. The optimum load resistance obtained in this study was 9600 Ω. The voltage increases with load, though slightly beyond 15 kΩ. It is worth noting that, the optimum value of load resistance for maximum power is affected by factors such as capacitance, frequency, damping ratio, etc. This result shows that load matching is very necessary for piezoelectric energy harvesting.

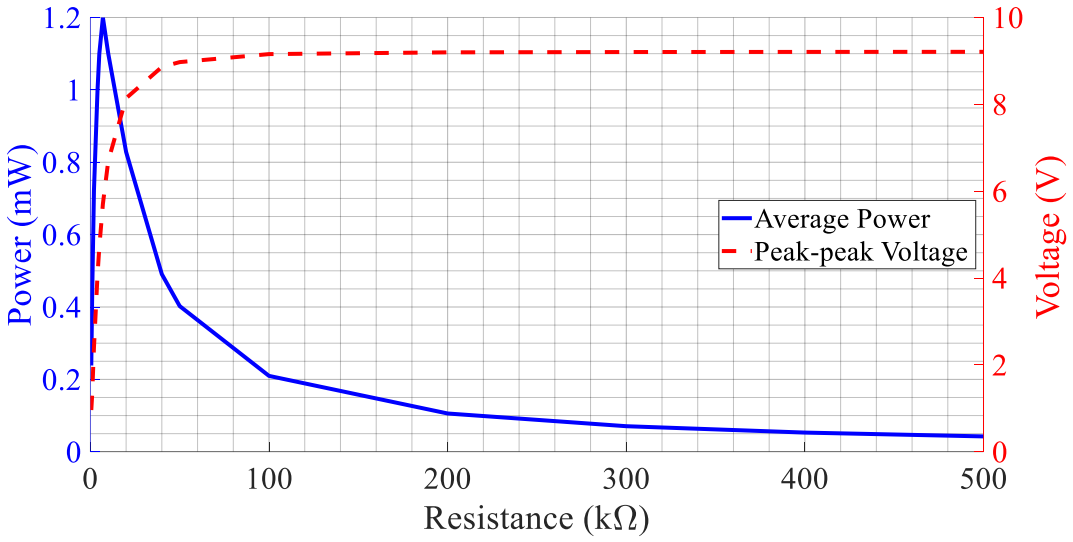

Figure 4.3 Results for power and peak-peak voltage vs load resistance at 0.04T. Note the direction of the arrows corresponding to the appropriate y-axis

4.2. Effect of Size of the Magnet on the Generated Voltage and Displacement

One parameter that affects the damping coefficient of the fluid is the radius of the magnet. As the size of the magnet greatly affects the damping of the piezoelectric cantilever beam, it is required to select a magnet with a reasonably small size. The size of the magnet chosen for this study was 2 mm in radius and this is was carefully selected to minimize the damping

effect of the fluid on the performance of the piezoelectric energy harvester and also ensuring it is practically tenable. In vibration energy harvesting, it is a requirement to minimize the mechanical damping as much as possible. In Fig. 4.4, it is seen that increasing the radius of the magnet decreases the displacement of the beam and the output voltage. This is because of the increase in damping as the radius of the magnet increases. This essentially means that the volume of fluid used greatly affects the performance of the piezoelectric energy harvesting system. This can be observed in Equation (3.8). It is also worth noting that the point of zero radius is the case of no fluid condition as the damping force shown in Equation (3.8) goes to zero at zero radius.

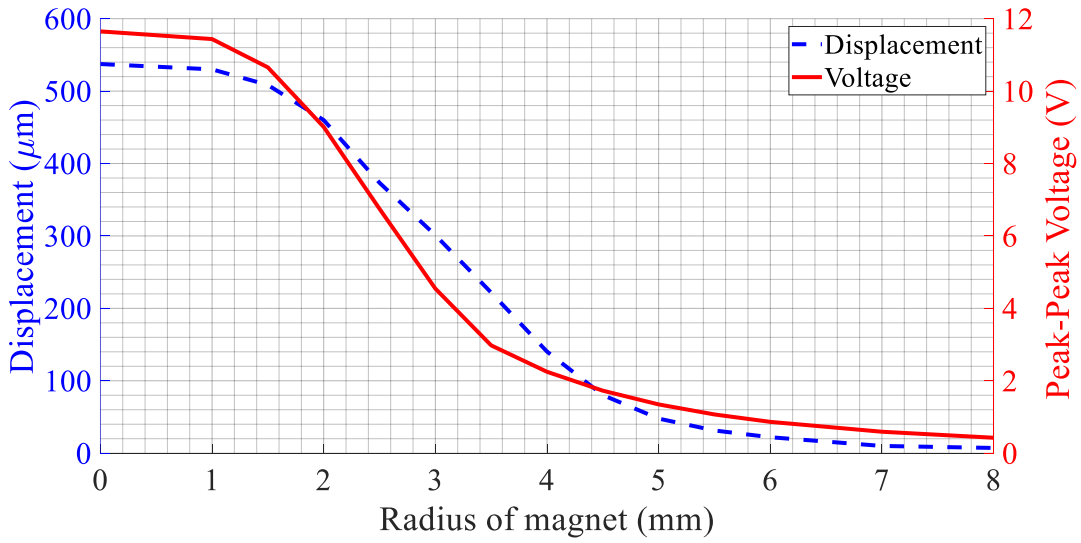

Figure 4.4 Results for displacement and voltage vs radius of the magnet. Note the direction of the arrows corresponding to the appropriate y-axis

4.3. Effect of Magnetic Field on the Output Voltage and Power

The magnetic field is the most important parameter in this thesis as it defines how the use of the fluid affects the performance of the piezoelectric energy harvester. The magnetic field is required to solidify the fluid

Figure 4.5 shows the voltage and power output of the piezoelectric energy harvester versus the magnetic field. As stated early, increasing the magnetic field increases the output voltage and hence, the power output of the piezoelectric energy harvester. This increase is because the mechanical damping ratio is inversely related to the frequency, hence increasing the magnetic field acting on the fluid solidifies the fluid more and increases the frequency of the beam due to stiffness increase leading to an increase in the power output. Fig. 4.5 shows that the fluid saturates at a magnetic field of 1.0 T. The voltage or power harvested beyond this value remains almost constant.

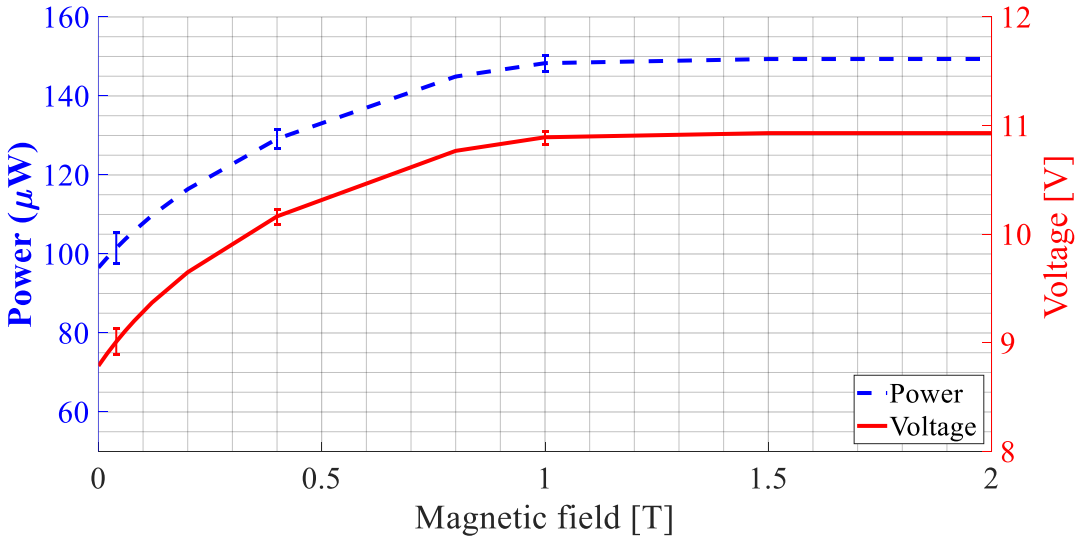

Figure 4.5 Variation of voltage and power output vs magnetic field. Note the direction of the arrows corresponding to the appropriate y-axis

4.4. Effect of Magnetic Field on the Vibrating Frequency of the Piezoelectric Beam

To study how the magnetic field influences the frequency of the device, the dynamic equations were parametrically solved for a range of magnetic field densities. Different magnet field adds different stiffness to the piezoelectric cantilever beam upon. The addition of the stiffness due to the fluid enhances the frequency of vibration of the beam.

The frequency enhancement capability of the fluid is displayed in Fig. 4.7. Increasing the magnetic field increases the stiffness of the piezoelectric beam when it comes into contact with the solidified fluid. This increases the frequency of vibration of the piezoelectric beam. The frequency is almost constant at the magnetic field of 1.0 T because of the saturation of the fluid beyond that field.

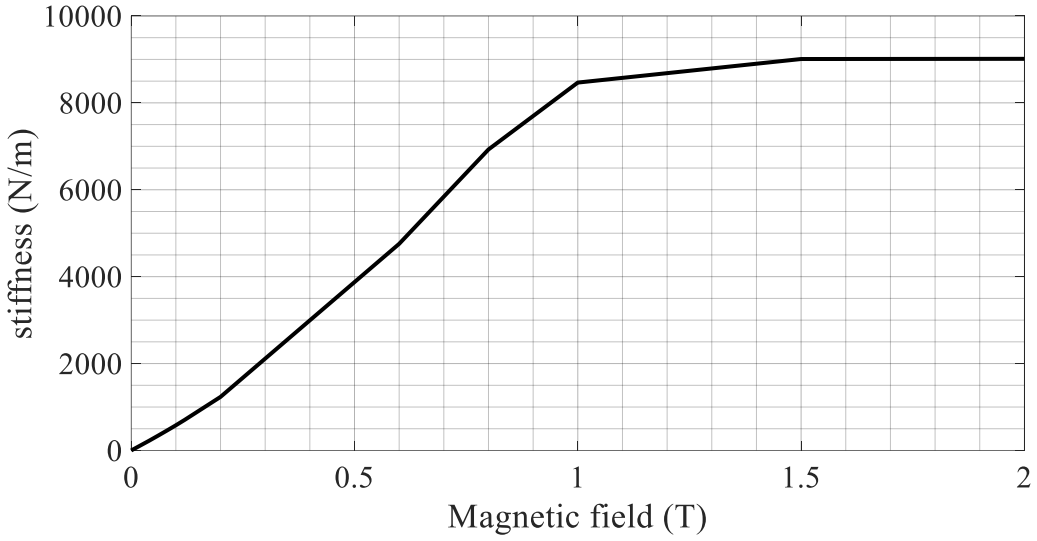

Figure 4.6 Stiffness due to the fluid at different magnetic field densities

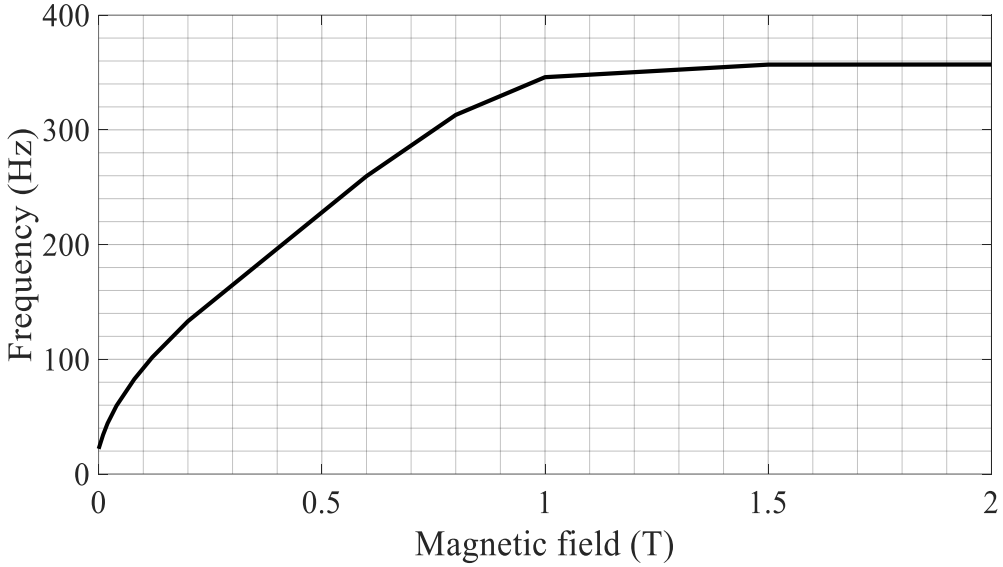

Figure 4.7 A plot of frequency vs magnetic field of the energy harvester

4.5. Frequency Response of the Proposed Energy Harvester

This subsection presents different results of the proposed system at varying frequencies. To study the frequency response of the piezoelectric energy harvester, the coupled single degree of freedom model is solved for different frequencies and the results for various parameters are extracted for discussion.

4.5.1. Displacement versus frequency results

The displacement response of the energy harvester is obtained through frequency parametric sweeps and by solving the theoretical SDOF using the MATLAB differential equation solver for different magnetic fields. The amplitude of the displacement is an

indication of the energy dissipation in the system and it is, therefore, considered an important parameter in vibration energy harvesting. The displacement of the piezoelectric cantilever beam versus frequency obtained when it is subjected to a constant sinusoidal input is shown in Fig. 4.8. With the application of the fluid at a magnetic field density of 0.04 T, the maximum displacement was obtained to be 0.5498 mm, and this drops marginally to 0.5270 mm at 0.08T and 0.5152 mm at 0.12 T. The decrease in displacement is attributed to damping due to the fluid and the additional spring constant added to the beam implies that the force applied to deflect the beam will have to increase correspondingly. Also, observed is the shift in the profile of the results indicating the change in frequency as a result of the change in the magnetic field. Increasing the magnetic field increases the frequency.

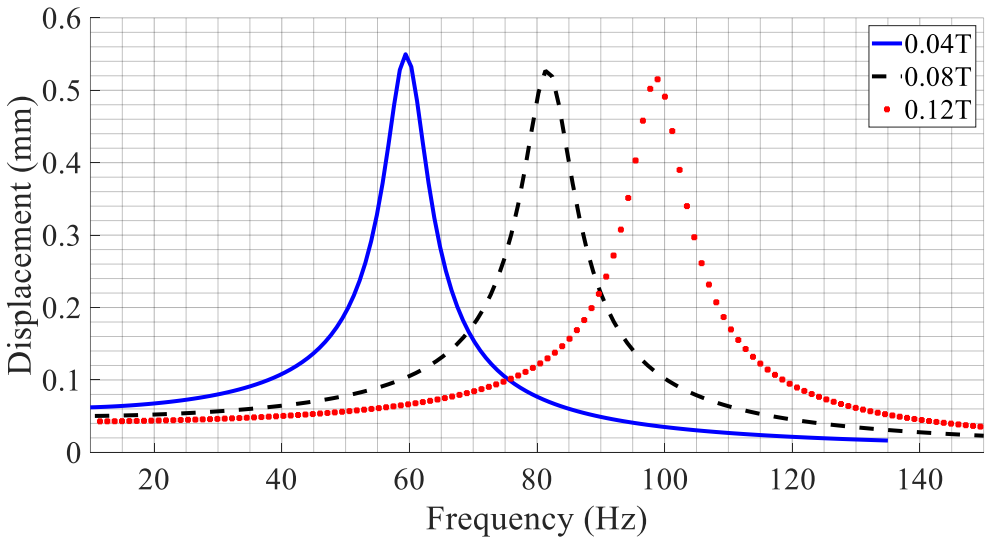

Figure 4.8 Displacement vs frequency of the piezoelectric cantilever beam at different frequencies

4.5.2. Stiffness and damping of MR fluid versus frequency

The displacement dependent squeeze mode damping and spring effect of the fluid can also be studied by using the results of the damping coefficient and stiffness due to the fluid. Again, to achieve this, the theoretical equations were solved for different magnetic fields with sinusoidal input frequencies of 10-150 Hz. The spring constants and damping coefficients due to the fluid were then computed. The results obtained in this study are depicted in Fig. 4.9 and Fig. 4.10.

The stiffness added to the piezoelectric beam for the different frequency of excitations and magnetic fields of 0.04 T, 0.08 T and 0.12 T are shown in Fig. 4.9. Increasing the magnetic field increases the solidification effect of the fluid as reported earlier in subsection 4.4. This increases the frequency of the beam. For different frequency of excitations, the stiffness of the MR fluid decreases as the vibration approaches resonance and increases sharply beyond the resonant frequency. In Fig. 4.9, the stiffness drops from 223 N/m at 10 Hz to 219 N/m at 59Hz and increases from the 219 N/m to about 223 N/m at 150 Hz. Clearly, it can be seen that the resonant frequency at this magnetic field of 0.04 T is 59 Hz. Again, for a magnetic field of 0.08 T, the stiffness drops from 457 to 450 N/m within the frequency range of 10-81 Hz and increases from the 450 to about 457 Hz at 150 Hz. The same trend is shown in the case of the 0.12 T magnetic field. Generally, the stiffness increases in amplitude as magnetic field increases. This trend is attributed to the fact that the beam vibrates at high frequency at resonance. Additionally, this is observed in the inverse correlation between the damping force and displacement in the model used.

Furthermore, the damping due to the fluid is studied under the same conditions as the stiffness. The damping coefficient of the fluid versus frequency for the different magnetic fields is reported in Fig. 4.10. The damping coefficient follows the same trend as the stiffness albeit not very much affected by the frequency change. For example, at a magnetic field of 0.04 T, the damping coefficient changes from 0.1804 Ns/m to 0.1759 Ns/m as the frequency increases from 10 Hz to 59 Hz. Thus, the damping coefficient decreases at resonance. It is also seen that the damping coefficient of the fluid is not greatly affected by the change in the magnetic field because the main parameter of the fluid which is dependent on the magnetic field is the yield stress. The damping force, however, is independent of the yield stress. Thus, by changing the magnetic field, the damping force is altered less significantly than the spring force generated when there is an impact. The stiffness due to the fluid is much sensitive to frequency changes as compared to the damping effect. This is due to the predominance of the spring component of the total force due to the fluid over the damping force because of the magnetic field yield dependent stress in the spring component of the total force due to the fluid.

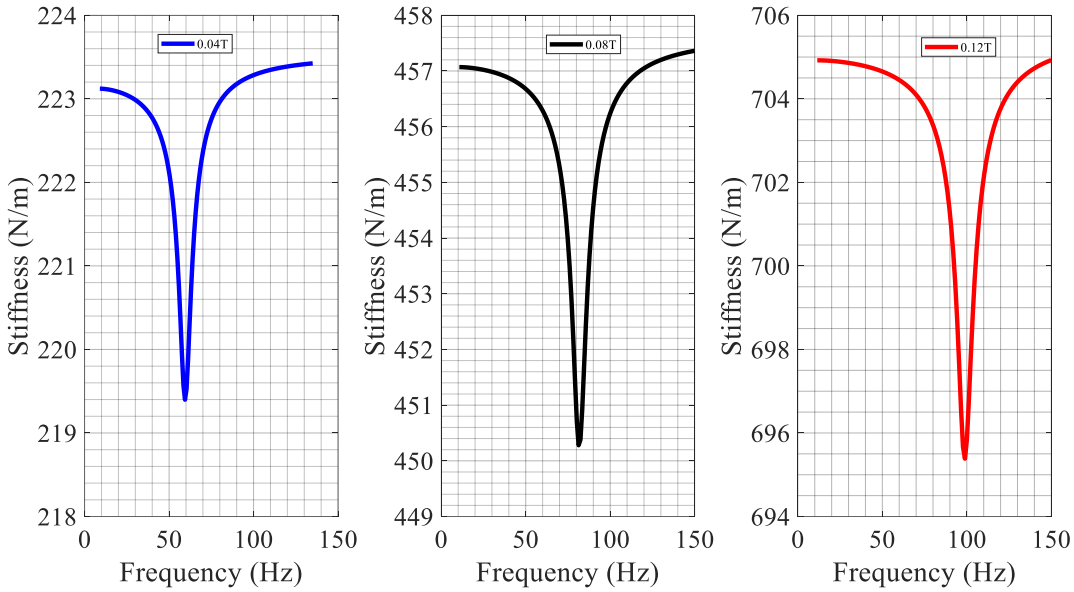

Figure 4.9 Stiffness of fluid vs frequency at different magnetic fields

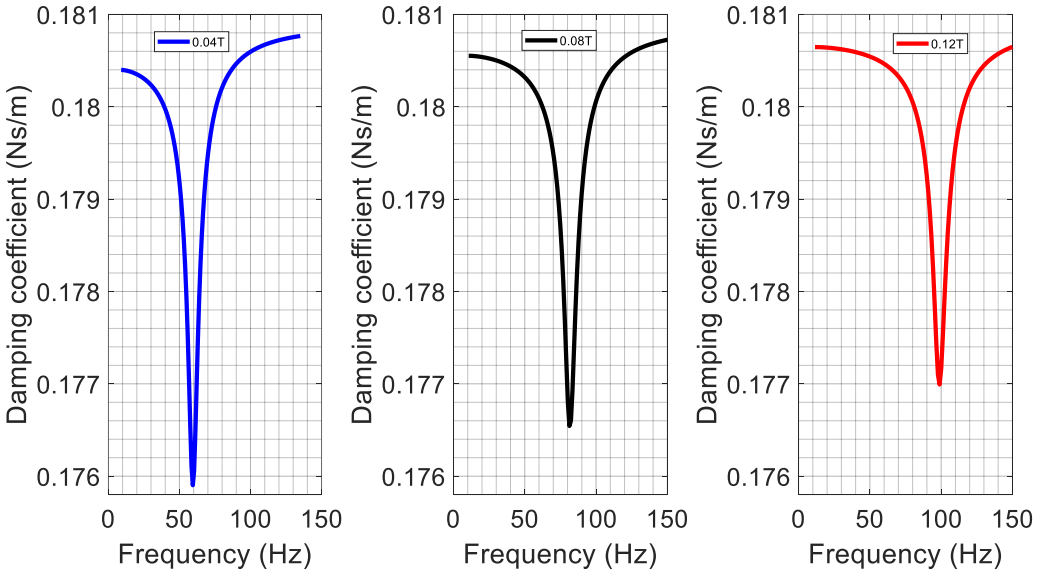

Figure 4.10 Damping coefficient vs frequency at different magnetic fields

4.5.3. Generated voltage versus frequency

The voltage across the load resistance is simulated for different frequencies and magnetic fields and the results are displayed in Fig. 4.11. Increasing the magnetic field increases the voltage drop across the load resistance and the corresponding frequency shift indicating the frequency change due to an overall stiffness increase of the piezoelectric beam when it impacts the fluid. As it is clearly seen, the maximum attainable voltage occurs when the frequency of the piezoelectric beam matches that of the excitation source. Vibrations in the environment typically have low frequencies and high amplitudes. Examples are those found in human motion such as walking, running, etc. [147], [56]. These types of energy converters operating with low resonant frequencies have low power transduction efficiencies [148]. The electromechanical conversion efficiency, φ, is given by $\frac{\varsigma_e}{\varsigma_e+\varsigma_m}$, where ς_e represents the electrical damping ratio and ς_m represents the mechanical damping ratio, is inversely related to frequency. This means converting mechanical power to electrical power reduces as the frequency decreases [149]. This goes to buttress the case of the voltage increase as the frequency is increased.

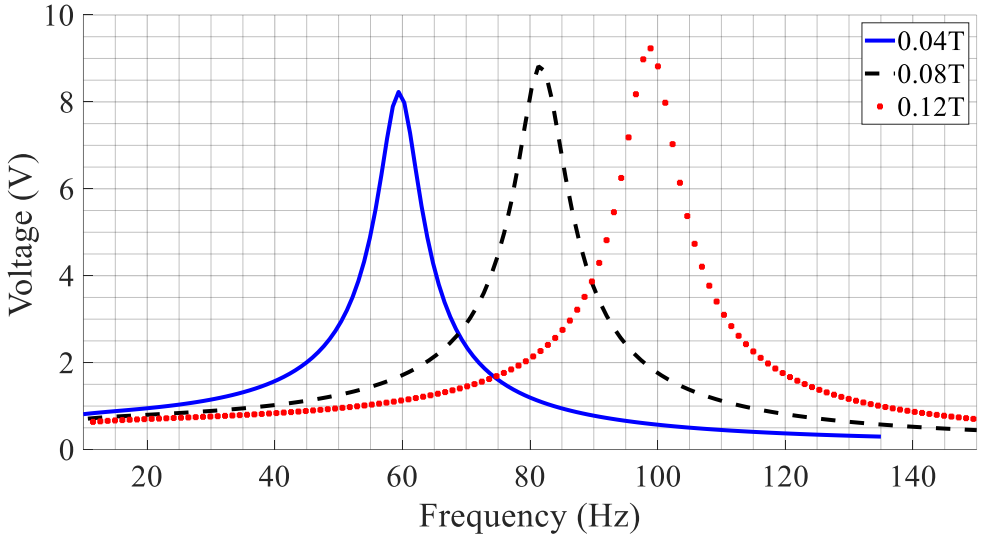

Figure 4.11 Generated voltage vs frequency at different magnetic fields

4.5.4. Power generated versus frequency

As stated earlier, piezoelectric cantilever beams convert mechanical strain into electrical voltage. When a load is connected to their terminals, electric current is generated. For a given piezoelectric coupling coefficient, the amount of power generated directly depends on the mechanical displacement and frequency of the piezoelectric beam. This means the piezoelectric cantilever beam should be made to deflect as much as possible. The deflection, however, is always limited by volume constraints, the strength of the vibration source, parasitic damping, and even the electric load connected across its terminal also causes damping.

It should be emphasized that energy harvesting from vibration is achieved through damping. Thus, the theory of vibration energy harvesting is the same as vibration attenuation. When it comes to energy harvesting, however, the mechanical damping ratio

should be carefully chosen to match the electrical damping (which increases with the load resistance) and should be as small as possible [5]. The power-frequency response of the proposed energy harvester was obtained by solving the theoretical equations. As stated earlier, piezoelectric devices produce maximum power at maximum strain/deflection. To produce useful power without any significant increase in displacement, the frequency of vibration is usually converted to a higher frequency to reduce the mechanical damping ratio as it is inversely related to frequency.

The results shown in Fig. 4.12, where the power increases marginally from 0.228 mW at 59 Hz with a magnetic field of 0.04T to 0.242 mW at 81 Hz when the magnetic field is increased to 0.08T. The power at 0.12T is seen to increase to 0.251 mW from the previous value. This power increase is due to the increase in frequency which offsets the additional damping added to the beam due to the use of the fluid.

Piezoelectric energy harvesters are resonant devices which are confirmed from the power results with the bell-shaped profile. Vibrations in the natural environment have varying frequencies. Vibration energy harvesters, therefore, require frequency matching mechanisms incorporated into them to constantly match the frequency of the transducer with the source. By changing the magnetic field to the fluid, the proposed energy generator frequency can be altered to match the excitation frequency of the source as it varies from 10 Hz to 150 Hz.

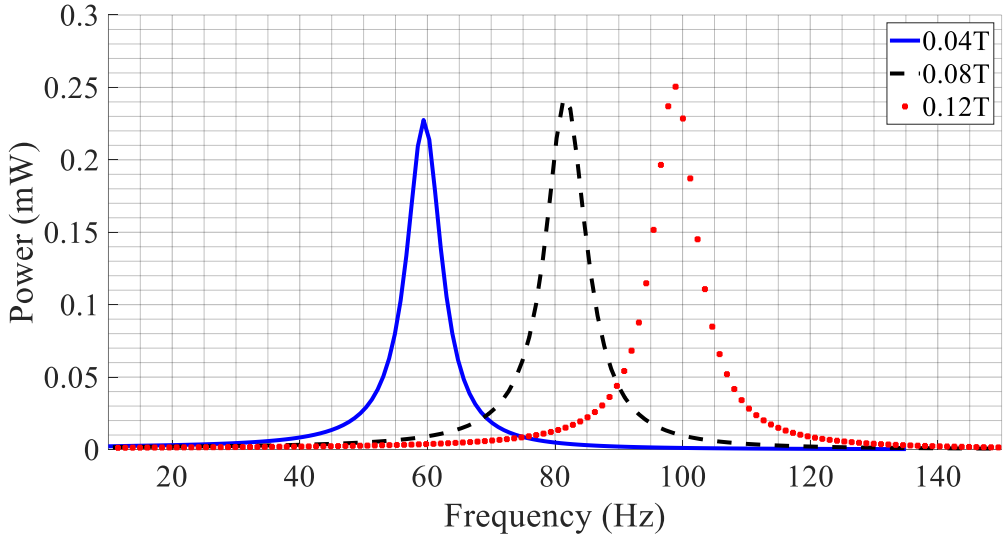

Figure 4.12 Power generated vs frequency at different magnetic fields

The results for the frequency response studies are summarised in the table below. It should be noted that, the values of the damping coefficient and stiffness due to the fluid are amplitudes taking with respect to the point of resonance, which has the minimum values. This was done to show how the stiffness increases but damping decreases with increasing magnetic field intensity.

Table 4.2 Summary of results for frequency response study

Magnetic field (T)	Stiffness due MRF (N/m)	Resonant frequency (Hz)	Damping coefficient of MRF (N.s/m)	Displacement (mm)	Voltage (V)	Power
0.040	4.100	59.400	0.005	0.550	8.232	0.228
0.080	7.100	81.320	0.004	0.527	8.824	0.242
0.120	9.800	98.900	0.003	0.515	9.234	0.251

Chapter 5: Conclusion and Recommendation

This study extended the application area of magnetorheological fluids, which have mostly been confined to vibration control in machinery and civil engineering structures. The present work was driven by the omnipresent use of Magnetorheological fluid devices without the necessary technologies to transduce the energy that is normally absorbed by dampers into a useable form.

The study focused on the design of a piezoelectric energy harvester using an MR fluid as a soft impact object to enhance the frequency of the system. The energy harvester presented here works based on the squeezing effect of an MR fluid. The squeeze force is produced when the vibrating beam impacts the fluid. The force generated upon consists of two components, which are the damping and stiffness components. The effects of these two forces for different magnetic fields were examined by simulating the dynamic equations and validating the simulation results experimentally. The results obtained from both studies were shown to agree. By varying the magnetic field, the results for the output voltage, power, and the frequency of the piezoelectric energy harvester could be enhanced. The results obtained showed the output voltage increased from 9.29 V at 0.04 T to 9.46 V at 0.08T for the numerical simulation and from 7.71V at 0.44 T to 8.46 V at 0.085 T for the experimental study. In addition, the frequency increased from 59.58 Hz to 82.76 Hz for the simulation and 61.02 Hz to 83.04 Hz for the experimental study.

The concept presented in this thesis is more beneficial than the solid-solid impact-based frequency up-conversion methods reported in the literature. This technique can tune the frequency while having the potential to minimize buckling and fatigue of the piezoelectric

cantilever beam due to impact. Moreover, the Heaviside function is employed to model the impact energy harvesting system. This more accurately captures the time-delay caused by the sticky and inelastic nature of the impact.

5.1. Summary of Results

The study in this thesis accomplished the following:

1. Compared experimental and numerical results of a piezoelectric energy harvesting system using a thin layer of MR fluid as an impact mechanism. The results from both the experimental and numerical were shown to be in good agreement.
2. Demonstrated that increasing the magnetic field applied to the fluid increased the generated voltage of the piezoelectric device.
3. Showed that the size of the magnet could greatly affect the performance of the piezoelectric harvester.
4. Illustrated the use of the fluid enhanced the operating frequency of the energy harvester.

5.2. Contribution

This thesis work presented a novel technique of enhancing the performance of a vibration-based piezoelectric energy generator using smart magnetorheological fluid as an impact mechanism. Smart fluids are currently an integral part of the automotive industry and the desire to make magnetorheological-based devices self-powered makes the contribution in

this thesis very paramount. A soft impact frequency up-conversion system has been presented for the first time in this thesis to minimise buckling of the piezoelectric beam as against the conventional techniques of using solid-solid impact mechanisms available in the literature. The Heaviside function has also been employed to model the nonlinear coupled behavior of the dynamic impact.

5.3. Recommendation for Future Work

The work presented here lays the foundation for more studies into the feasibility of the proposed concept. One of the advantages of using the fluid as an impact object in the study is to reduce buckling and fatigue of the piezoelectric beam due to the impact. Further work based on fatigue analysis and buckling of the piezoelectric due to the impact is, therefore, required to ascertain how much protection the fluid offers to the beam. This will provide a great comparison with the existing solid-solid impact-based systems proposed in the literature.

The present study still needs optimization of several parameters. Parameter estimation should be performed to determine the best parameters for the proposed design. Future studies should concentrate on parameter estimation.

Finally, a prototype design will also lend more credence to the proposed concept based on the results of the parameter estimation.

5.4. List of Publications

The following are some of the published works of my studies:

1. **H. Azangbebil**, S. S. Djokoto, and M. Agelin-Chaab, (in press), "Experimental and numerical studies of a soft impact piezoelectric energy harvesting using an MR fluid," IEEE Sensor Journal, 2020.
2. S. S. Djokoto, **H. Azangbebil**, M. Agelin-Chaab, E. Dragašius, and V. Jūrėnas, "Modeling and study of magnetorheological fluid impact base frequency enhancement for a micro-piezoelectric energy generator," Int. J. Green Energy, vol. 17, no. 9, pp. 529–539, 2020.
3. **H. Azangbebil**, S. S. Djokoto, M. Agelin-Chaab, and E. Dragašius, "A Study of Nonlinear Piezoelectric Energy Harvester with Variable Damping using Thin Film MR Fluid," in IFAC-PapersOnLine, 2019, vol. 52, no. 10, pp. 394–399.
4. S. S. Djokoto, **H. Azangbebil**, M. Agelin-chaab, E. Dragasius, and V. Jurenas, "Design and Modeling of MRF Impact Base Frequency Enhancement for a Piezoelectric Energy Generator," in CSME-CFDSC Congress, 2019.

REFERENCES

[1] B. Kathpalia, “Methods of piezoelectric energy harvesting from human body motions,” MSc. thesis, Georgia Institute of Technology, 2018.

[2] J. Bryzek *et al.*, “Marvelous MEMs: Advanced IC sensors and microstructures for high volume applications,” *IEEE Circuits Devices Mag.*, vol. 22, no. 2, pp. 8–28, 2006.

[3] F. Yildiz and K. L. Coogler, “Low power energy harvesting with a thermoelectric generator through an air conditioning condenser,” *J. Eng. Technol.*, vol. 34, no. 1, pp. 8–16, 2017.

[4] I. Sil, S. Mukherjee, and K. Biswas, “A review of energy harvesting technology and its potential applications,” *Environ. Earth Sci. Res. J.*, vol. 4, no. 2, pp. 33–38, 2017.

[5] S. Roundy, P. K. Wright, and J. Rabaey, “A study of low level vibrations as a power source for wireless sensor nodes,” *Comput. Commun.*, vol. 26, no. 11, pp. 1131–1144, 2003.

[6] S. Boisseau, G. Despesse, and B. Ahmed, “Electrostatic Conversion for Vibration Energy Harvesting,” in *Small-Scale Energy Harvesting*, 2012.

[7] A. R. El-Sayed, K. Tai, M. Biglarbegian, and S. Mahmud, “A survey on recent energy harvesting mechanisms,” *Can. Conf. Electr. Comput. Eng.*, vol. 2016-Octob, pp. 1–5, 2016.

[8] A. Erturk, “Electromechanical Modeling of Piezoelectric Energy Harvesters,” Ph.D. thesis, Virginia Polytechnic Institute and State University, 2009.

[9] A. Ulasyar and I. Lazoglu, “Design and analysis of a new magnetorheological damper for washing machine,” *J. Mech. Sci. Technol.*, vol. 32, no. 4, pp. 1549–1561, 2018.

[10] K. El Majdoub, D. Ghani, F. Giri, and F. Z. Chaoui, “Adaptive semi-active suspension of quarter-vehicle with magnetorheological damper,” *J. Dyn. Syst. Meas. Control. Trans. ASME*, vol. 137, no. 2, pp. 1–12, 2015.

[11] J. Koo, “Using Magneto-Rheological Dampers in Semiactive Tuned Vibration Absorbers to Control Structural Vibrations,” Ph.D. thesis, Virginia Polytechnic Institute and State University, 2003.

[12] V. Lara-Prieto, R. Parkin, M. Jackson, V. Silberschmidt, and Z. Kęsy, “Vibration characteristics of MR cantilever sandwich beams: Experimental study,” *Smart Mater. Struct.*, vol. 19, no. 1, 2010.

[13] G. Sun, G. Qiao, and B. Xu, “Corrosion monitoring sensor networks with energy harvesting,” *IEEE Sens. J.*, vol. 11, no. 6, pp. 1476–1477, 2011.

[14] M. Okayasu and T. Yamasaki, “Structural Health Monitoring System for Remote Inspection of Material Failure,” *J. Nondestruct. Eval.*, vol. 38, no. 2, pp. 1–6, Jun.

2019.

[15] W. W. Clark, J. R. Romeiko, D. A. Charnegie, G. Kusic, and C. Mo, “A case study in energy harvesting for powering a wireless measurement system,” in *6th International Workshop on Structural Health Monitoring*, 2007, vol. 2, pp. 1765–1772.

[16] D. Tomicek, Y. H. Tham, W. K. G. Seah, and R. K. Rayudu, “Vibration-powered wireless sensor for structural monitoring during earthquakes,” in *Proceedings of the 6th International Conference on Structural Health Monitoring of Intelligent Infrastructure*, 2013.

[17] D. Dondi, G. Napoletano, A. Bertacchini, L. Larcher, and P. Pavan, “A WSN system powered by vibrations to improve safety of machinery with trailer,” *Proc. IEEE Sensors*, pp. 1–4, 2012.

[18] A. Moure *et al.*, “Feasible integration in asphalt of piezoelectric cymbals for vibration energy harvesting,” *Energy Convers. Manag.*, vol. 112, pp. 246–253, Mar. 2016.

[19] M. Wischke, M. Masur, M. Kröner, and P. Woias, “Vibration harvesting in traffic tunnels to power wireless sensor nodes,” *Smart Mater. Struct.*, vol. 20, no. 8, 2011.

[20] H.-J. Jung, I.-H. Kim, and J. Park, “Experimental validation of energy harvesting device for civil engineering applications,” *Sensors Smart Struct. Technol. Civil, Mech. Aerosp. Syst. 2012*, vol. 8345, no. April 2012, p. 83451C, 2012.

[21] I. H. Kim, S. J. Jang, and H. J. Jung, “Performance enhancement of a rotational energy harvester utilizing wind-induced vibration of an inclined stay cable,” *Smart Mater. Struct.*, vol. 22, no. 7, 2013.

[22] D. Dumas, F. Lani, T. Monnier, R. Smaili, and J. Loyer, “Damage detection in composite structures using autonomous wireless systems: Simulation & validation,” *J. Phys. Conf. Ser.*, vol. 305, no. 1, 2011.

[23] T. Starner, “Human Powered wearable,” *Ibm Syst. J.*, vol. 35, no. 3, 1996.

[24] Freeplay Energy, “Innovative energy solutions for the world,” 2013. [Online]. Available: http://www.freeplayenergy.com/. [Accessed: 10-Apr-2020].

[25] Seiko Corp., “PARTS CATALOGUE / TECHNICAL GUIDE Cal. 5M62A, 5M63A.” pp. 1–12.

[26] P. Pillatsch, “Piezoelectric Energy Harvesting From Low Frequency And Random Excitation Using Frequency Up-Conversion,” Ph.D. thesis, Imperial Colege London, 2013.

[27] “Applied Innovative Technologies, Inc. (AIT) | Advancing Light and Power Technology.” [Online]. Available: https://appliedinnotech.wordpress.com/. [Accessed: 30-Apr-2020].

[28] J. Kymissis, C. Kendall, J. Paradiso, and N. Gershenfeld, “Parasitic power

harvesting in shoes," *Int. Symp. Wearable Comput. Dig. Pap.*, vol. 1998-Octob, pp. 132–139, 1998.

[29] J. G. Rocha, L. M. Gonçalves, P. F. Rocha, M. P. Silva, and S. Lanceros-Méndez, "Energy harvesting from piezoelectric materials fully integrated in footwear," *IEEE Trans. Ind. Electron.*, vol. 57, no. 3, pp. 813–819, 2010.

[30] L. Xie and M. Cai, "Increased piezoelectric energy harvesting from human footstep motion by using an amplification mechanism," *Appl. Phys. Lett.*, vol. 105, no. 14, p. 143901, Oct. 2014.

[31] D. Ma, G. Lan, W. Xu, M. Hassan, and W. Hu, "Poster: Unobtrusive user verification using piezoelectric energy harvesting," in *ACM International Conference Proceeding Series*, 2017, pp. 541–542.

[32] J. Granstrom, J. Feenstra, H. A. Sodano, and K. Farinholt, "Energy harvesting from a backpack instrumented with piezoelectric shoulder straps," *Smart Mater. Struct.*, vol. 16, no. 5, pp. 1810–1820, 2007.

[33] S. Almouahed, M. Gouriou, C. Hamitouche, E. Stindel, and C. Roux, "The use of piezoceramics as electrical energy harvesters within instrumented knee implant during walking," *IEEE/ASME Trans. Mechatronics*, vol. 16, no. 5, pp. 799–807, 2011.

[34] J. Holmberg, L. Alexander, R. Rajamani, and J. E. Bechtold, "Battery-less wireless instrumented knee implant," *J. Med. Devices, Trans. ASME*, vol. 7, no. 1, 2013.

[35] M. Safaei, R. M. Meneghini, and S. R. Anton, "Force detection, center of pressure tracking, and energy harvesting from a piezoelectric knee implant," *Smart Mater. Struct.*, vol. 27, no. 11, p. 114007, Sep. 2018.

[36] S. Khalifa, G. Lan, and S. Member, "HARKE : Human Activity Recognition from Kinetic Energy Harvesting Data in Wearable Devices," *IEEE Trans. Mob. Comput.*, vol. 17, no. 6, pp. 1353–1368, 2018.

[37] M. Deterre, E. Lefeuvre, Y. Zhu, M. Woytasik, B. Boutaud, and R. D. Molin, "Micro blood pressure energy harvester for intracardiac pacemaker," *J. Microelectromechanical Syst.*, vol. 23, no. 3, pp. 651–660, 2014.

[38] M. A. Karami and D. J. Inman, "Powering pacemakers from heartbeat vibrations using linear and nonlinear energy harvesters," *Appl. Phys. Lett.*, vol. 100, no. 4, pp. 0003–6951, 2012.

[39] G. T. Hwang *et al.*, "Self-powered cardiac pacemaker enabled by flexible single crystalline PMN-PT piezoelectric energy harvester," *Adv. Mater.*, vol. 26, no. 28, pp. 4880–4887, Jul. 2014.

[40] T. Reissman and E. Garcia, "An ultra-lightweight multi-source power harvesting system for insect cyborg sentinels," in *Proceedings of the ASME Conference on Smart Materials, Adaptive Structures and Intelligent Systems, SMASIS2008*, 2008, vol. 2, pp. 711–718.

[41] M. W. Shafer, R. MacCurdy, E. Garcia, and D. Winkler, “Harvestable vibrational energy from an avian source: theoretical predictions vs. measured values,” *Act. Passiv. Smart Struct. Integr. Syst. 2012*, vol. 8341, no. March 2012, p. 834103, 2012.

[42] M. W. Shafer and E. Morgan, “Energy Harvesting for Marine-Wildlife Monitoring,” in *ASME Conference on Smart Materials, Adaptive Structures and Intelligent Systems*, 2014.

[43] C. S. Brownt, R. C. Kellt, and A. X. D. L. A. Thomas, “Piezoelectric Materials , A Review of Progress,” *IEEE Trans. Compon. Parts*, vol. 109, no. 43, pp. 99–114, 1962.

[44] G. Lippmann, “Principe de la conservation de l’électricité, ou second principe de la théorie des phénomènes électriques,” *J. Phys. Theor. Appl*, vol. 1881, no. 1, pp. 381–394.

[45] S. Priya and D. J. Inman, *Energy Harvesting Technologies*. Springer, 2009.

[46] W. Al-Ashtari, M. Hunstig, T. Hemsel, and W. Sextro, “Frequency tuning of piezoelectric energy harvesters by magnetic force,” *Smart Mater. Struct.*, vol. 21, no. 3, 2012.

[47] D. Zhu, M. J. Tudor, and S. P. Beeby, “Strategies for increasing the operating frequency range of vibration energy harvesters: A review,” *Meas. Sci. Technol.*, vol. 21, no. 2, 2010.

[48] R. D. Blevins, *Formulas-for-Natural-Frequency-and-Mode-Shape*. .

[49] J. F. Gieras, J.-H. Oh, M. Huzmezan, and H. S. Sane, “Electromechanical Energy Harvesting System,” WO2007070022(A2), WO2007070022(A3), 2007.

[50] X. Wu, J. Lin, S. Kato, K. Zhang, T. Ren, and L. Liu, “A Frequency adjustable vibration energy harvester,” in *Proceedings of PowerMEMS 2008 & microEMS2008*, 2008, pp. 9–12.

[51] V. R. Challa, M. G. Prasad, Y. Shi, and F. T. Fisher, “A vibration energy harvesting device with bidirectional resonance frequency tunability,” *Smart Mater. Struct.*, vol. 17, no. 1, 2008.

[52] C. Eichhorn, F. Goldschmidtboeing, and P. Woias, “Bidirectional frequency tuning of a piezoelectric energy converter based on a cantilever beam,” *J. Micromechanics Microengineering*, vol. 19, no. 9, 2009.

[53] S. M. Shahruz, “Design of mechanical band-pass filters for energy scavenging,” *J. Sound Vib.*, vol. 292, no. 3–5, pp. 987–998, May 2006.

[54] S. Zhou, J. Cao, A. Erturk, and J. Lin, “Enhanced broadband piezoelectric energy harvesting using rotatable magnets,” *Appl. Phys. Lett.*, vol. 102, no. 17, pp. 1–5, 2013.

[55] M. Umeda, K. Nakamura, and S. Ueha, “Energy Storage Characteristics of a

Piezo- Generator using Impact Induced Vibration," *Jpn. J. Appl. Phys.*, vol. 36, pp. 3146–3151, 1997.

[56] M. A. Halim, S. Khym, and J. Y. Park, "Impact based frequency increased piezoelectric vibration energy harvester for human motion related environments," in *8th Annual IEEE International Conference on Nano/Micro Engineered and Molecular Systems, IEEE NEMS 2013*, 2013, pp. 949–952.

[57] S. S. Djokoto, H. Azangbebil, M. Agelin-chaab, E. Dragasius, and V. Jurenas, "Design and Modeling of MRF Impact Base Frequency Enhancement for a Piezoelectric Energy Generator," in *CSME-CFDSC Congress*, 2019.

[58] S. Moss, A. Barry, I. Powlesland, S. Galea, and G. P. Carman, "A low profile vibro-impacting energy harvester with symmetrical stops," *Appl. Phys. Lett.*, vol. 97, no. 23, pp. 97–100, 2010.

[59] J. Zhang and L. Qin, "A tunable frequency up-conversion wideband piezoelectric vibration energy harvester for low-frequency variable environment using a novel impact- and rope-driven hybrid mechanism," *Appl. Energy*, vol. 240, no. January, pp. 26–34, 2019.

[60] H. Liu, C. Lee, T. Kobayashi, C. J. Tay, and C. Quan, "Investigation of a MEMS piezoelectric energy harvester system with a frequency-widened-bandwidth mechanism introduced by mechanical stoppers," *Smart Mater. Struct.*, vol. 21, no. 3, 2012.

[61] L. Gu and C. Livermore, "Impact-driven, frequency up-converting coupled vibration energy harvesting device for low frequency operation," *Smart Mater. Struct.*, vol. 20, no. 4, 2011.

[62] K. Melzner, J. Fleischer, and S. Odenbach, "New developments in the investigation of magnetoviscous and viscoelastic effects in magnetic fluids.," *Magnetohydrodyn. vol. 37, no. 3, p. 285-290*, vol. 37, pp. 285–290, 2001.

[63] W. M. Winslow, "Methods and means for translating electrical impulses into mechanical force," US Patent 2,417,850, 1947.

[64] J. Rabinov, "The magnetic fluid clutch," *AIEE Trans*, vol. 20, pp. 1308–1315, 1948.

[65] W. M. Winslow, "Induced fibration of suspensions," *J. Appl. Phys.*, vol. 20, pp. 1137–1140, 1949.

[66] S.-B. Choi and Y.-M. Han, *Magnetorheological Fluid Technology*. 2012.

[67] S. S. Djokoto, M. Agelin-Chaab, V. Jurenas, and E. Dragasius, "Experimental Investigation of Squeezed MRF Film Stopper and Its Effect on Vibrating Bimorph for Frequency Tuning of an Energy Generator," in *Conference Proceedings - IEEE SOUTHEASTCON*, 2019, pp. 1–7.

[68] Y. D. Liu and H. J. Choi, "Electrorheological fluids: Smart soft matter and characteristics," *Soft Matter*, vol. 8, no. 48, pp. 11961–11978, 2012.

[69] Lord Corporation, “MRF-132DG magneto-rheological fluid, Lord Technical Data Sheet, DS7015.” 2008.

[70] F. D. Goncalves and J. D. Carlson, “An alternate operation mode for MR fluids—magnetic gradient pinch,” *J. Phys. Conf. Ser.*, vol. 149, no. 1, p. 012050, Feb. 2009.

[71] J. D. Carlson and R. M. Jolly, “MR fluid, foam and elastomer devices,” *Phys. Lett. A*, vol. 114, no. 5, pp. 555–569, 2000.

[72] S. Kaluvan, K. Shah, and S. B. Choi, “A new resonant based measurement method for squeeze mode yield stress of magnetorheological fluids,” *Smart Mater. Struct.*, vol. 23, no. 11, 2014.

[73] B. Sapiński, W. Horak, and M. Szczech, “Investigation of MR fluids in the oscillatory squeeze mode,” *Acta Mech. Autom.*, vol. 7, no. 2, pp. 111–116, 2013.

[74] M. T. Avraam, “MR-fluid brake design and its application to a portable muscular rehabilitation device,” PhD thesis, Universite` Libre De Bruxelles, 2009.

[75] G. Yang, B. F. Spencer, J. D. Carlson, and M. K. Sain, “Large-scale MR fluid dampers: Modeling and dynamic performance considerations,” *Eng. Struct.*, vol. 24, no. 3, pp. 309–323, 2002.

[76] X. Zhu, X. Jing, and L. Cheng, “Magnetorheological fluid dampers: A review on structure design and analysis,” *Journal of Intelligent Material Systems and Structures*, vol. 23, no. 8. pp. 839–873, 2012.

[77] E. Guglielmino, T. Sireteanu, C. W. Stammers, and M. Giuclea, *Semi-active Suspension Control: Improved Vehicle Ride and Road Friendliness*. London: Springer, 2008.

[78] B.-G. Kim, C. Han, S.-B. Choi, and B.-H. Kang, “Design and Analysis of a Magnetorheological Damper for Airplane Landing Gear,” in *SPIE Smart Structures and Materials + Nondestructive Evaluation and Health Monitoring*, 2018.

[79] D. V. A. Ramasastry, K. V. Ramana, N. M. Rao, S. S. Kumar, and T. G. L. Priyanka, “Analysis of Train Suspension System Using MR dampers,” in *IOP Conference Series: Materials Science and Engineering*, 2016, vol. 149, no. 1.

[80] H. J. Singh and N. M. Wereley, “Optimal control of gun recoil in direct fire using magnetorheological absorbers,” *Smart Mater. Struct.*, vol. 23, no. 5, 2014.

[81] S. Kaluvan and S. B. Choi, “Design of current sensor using a magnetorheological fluid in shear mode,” *Smart Mater. Struct.*, vol. 23, no. 12, 2014.

[82] N. Golinelli and A. Spaggiari, “Design of a novel magnetorheological damper with internal pressure control,” *Frat. ed Integrità Strutt. ed Integrità Strutt.*, vol. 9, no. 32, pp. 13–23, 2015.

[83] W. Liao, C. Chen, and H. Guo, “Magnetorheological Devices with Multiple

Functions," *Magnetorheol. Adv. Appl.*, no. 6, pp. 342–362, 2014.

[84] H. Du, K. Yim Sze, and J. Lam, "Semi-active H∞ control of vehicle suspension with magneto-rheological dampers," *J. Sound Vib.*, vol. 283, no. 3–5, pp. 981–996, 2005.

[85] G. Hu, Y. Lu, S. Sun, and W. Li, "Performance Analysis of a Magnetorheological Damper with Energy Harvesting Ability," *Shock Vib.*, vol. 2016, pp. 1–10, Aug. 2016.

[86] G. Xinchun, H. Yonghu, R. Yi, L. Hui, and O. Jinping, "A novel self-powered MR damper: Theoretical and experimental analysis," *Smart Mater. Struct.*, vol. 24, no. 10, 2015.

[87] B. Sapiński, "Energy-harvesting linear MR damper: Prototyping and testing," *Smart Mater. Struct.*, vol. 23, no. 3, 2014.

[88] C. Chen and W. H. Liao, "A self-sensing magnetorheological damper with power generation," *Smart Mater. Struct.*, vol. 21, no. 2, 2012.

[89] X. Bai, Q. Zou, and L. Qian, "Design and test of a power-generated magnetorheological damper," in *Active and Passive Smart Structures and Integrated Systems 2017*, 2017, vol. 10164, no. April 2017, p. 101641J.

[90] K. Nakano, Y. Suda, and S. Nakadai, "Self-powered active vibration control using a single electric actuator," *J. Sound Vib.*, vol. 260, no. 2, pp. 213–235, 2003.

[91] E. T. Tanner, M. Ahmadian, D. J. Leo, and D. K. Lindner, "Combined Shock and Vibration Isolation Through the Self-Powered, Semi-Active Control of a Magnetorheological Damper in Parallel with an Air Spring," *Shock Vib.*, 2003.

[92] B. Sapiński, M. Węgrzynowski, and J. Nabielec, "Magnetorheological damper–based positioning system with power generation," *J. Intell. Mater. Syst. Struct.*, vol. 29, no. 6, pp. 1236–1254, Apr. 2018.

[93] C. Chen, Y. S. Chan, L. Zou, and W.-H. Liao, "Self-powered magnetorheological dampers for motorcycle suspensions," *Proc. Inst. Mech. Eng. Part D J. Automob. Eng.*, vol. 232, no. 7, pp. 921–935, Jun. 2018.

[94] R. Ahamed, M. Rashid, M. Ferdaus, and H. B. Yusuf, "Modelling and performance evaluation of energy harvesting linear magnetorheological (MR) damper," *J. Low Freq. Noise, Vib. Act. Control*, vol. 36, no. 2, pp. 177–192, Jun. 2017.

[95] J. Yu, X. Dong, Z. Zhang, and P. Chen, "A novel scissor-type magnetorheological seat suspension system with self-sustainability," *J. Intell. Mater. Syst. Struct.*, vol. 30, no. 5, pp. 665–676, 2016.

[96] I.-H. Kim, H.-J. Jung, and J.-H. Koo, "Experimental evaluation of a self-powered smart damping system in reducing vibrations of a full-scale stay cable," *Smart Mater. Struct.*, vol. 19, no. 11, p. 115027, Nov. 2010.

[97] M. Yu, Y. Peng, S. Wang, J. Fu, and S. B. Choi, “A new energy-harvesting device system for wireless sensors, adaptable to on-site monitoring of MR damper motion,” *Smart Mater. Struct.*, vol. 23, no. 7, p. 077002, Jul. 2014.

[98] S. W. Or, Y. F. Duan, Y. Q. Ni, Z. H. Chen, and K. H. Lam, “Development of magnetorheological dampers with embedded piezoelectric force sensors for structural vibration control,” *J. Intell. Mater. Syst. Struct.*, vol. 19, no. 11, pp. 1327–1338, 2008.

[99] F. D. Goncalves, J.-H. Koo, and M. Ahmadian, “A review of the state of the art in magnetorheological fluid technologies - Part I: MR fluid and MR fluid models,” *Shock Vib. Dig.*, vol. 38, no. 3, pp. 203–219, May 2006.

[100] K. D. Weiss, J. D. Carlson, and D. A. Nixon, “Viscoelastic properties of magneto- and electro-rheological fluids,” *J. Intell. Mater. Syst. Struct.*, vol. 5, no. 6, pp. 772–775, Nov. 1994.

[101] C. Kormann, M. Laun, and G. Klett, “Actuators 94,” in *4th International Conference on New Actuators, eds. H. Borgmann and K. Lenz, Axon Technologies Consult GmbH, 271*, 1994.

[102] X. Wang and F. Gordaninejad, “Flow Analysis and Modeling of Field-Controllable, Electro- and Magneto-Rheological Fluid Dampers,” *J. Appl. Mech.*, vol. 74, no. 1, p. 13, 2007.

[103] Y. T. Choi, J. U. Cho, S. B. Choi, and N. M. Wereley, “Constitutive models of electrorheological and magnetorheological fluids using viscometers,” *Smart Mater. Struct.*, vol. 14, no. 5, pp. 1025–1036, Oct. 2005.

[104] R. Stanway, J. L. Sproston, and A. K. El-Wahed, “Applications of electro-rheological fluids in vibration control: a survey,” *Smart Mater. Struct.*, vol. 5, no. 4, pp. 464–482, Aug. 1996.

[105] K. C. Wilson and A. D. Thomas, “Analytic model of laminar-turbulent transition for Bingham plastics,” *Can. J. Chem. Eng.*, vol. 84, no. 5, pp. 520–520, Oct. 2006.

[106] D. H. Wang and W. H. Liao, “Magnetorheological fluid dampers: A review of parametric modelling,” *Smart Mater. Struct.*, vol. 20, no. 2, 2011.

[107] W. R. Philips, “Engineering Applications of Fluids with a Variable Yield Stress,” Ph.D. thesis, University of California, Berkeley, 1969.

[108] H. P. Gavin, “Electrorheological Dampers for Structural Vibration Suppression,” Ph.D. thesis, University of Michigan, 1994.

[109] R. Stanway, J. L. Sproston, and N. G. Stevens, “Non-Linear Modeling of an Electro-Rheological Vibration Damper,” *IFAC Proc. Vol.*, vol. 18, no. 5, pp. 195–200, 2017.

[110] N. M. Wereley and L. Pang, “Non-dimensional analysis of semi-active electrorheological and magnetorheological dampers using approximate parallel plate models,” *Smart Mater. Struct.*, vol. 7, no. 5, pp. 732–743, Oct. 1998.

[111] W. Hu and N. M. Wereley, “Non-dimensional Damping Analysis of Flow-Mode Magnetorheological and Electrorheological Dampers,” in *Aerospace*, 2008, vol. 2003, pp. 265–272.

[112] G. M. Kamath, M. K. Hurt, and N. M. Wereley, “Analysis and testing of Bingham plastic behavior in semi-active electrorheological fluid dampers,” *Smart Mater. Struct*, vol. 5, pp. 576–590, 1996.

[113] H. P. Gavin, R. D. Hanson, and F. E. Filisko, “Electrorheological Dampers, Part I: Analysis and Design,” *J. Appl. Mech.*, vol. 63, no. 3, p. 669, Sep. 1996.

[114] G. Yang, B. F. Spencer, J. D. Carlson, and M. K. Sain, “Large-scale MR fluid dampers: modeling and dynamic performance considerations,” *Eng. Struct.*, vol. 24, pp. 309–323, 2002.

[115] X. Wang and F. Gordaninejad, “Flow Analysis of Field-Controllable, Electro- and Magneto-Rheological Fluids Using Herschel-Bulkley Model,” *J. Intell. Mater. Syst. Struct.*, vol. 10, no. 8, pp. 601–608, Aug. 1999.

[116] D. Lee and N. M. Wereey, “Analysis of electro- and magneto-rheological flow mode dampers using Herschel-Bulkley model,” *Smart Struct. Mater.*, vol. 3989, no. 301, pp. 244–255, 2000.

[117] X. Wang and F. Gordaninejad, “Study of field-controllable, electro- and magneto-rheological fluid dampers in flow mode using Herschel-Bulkley theory,” in *SPIE’s 7th Annual International Symposium on Smart Structures and Materials, 2000*, 2003, vol. 3989, pp. 232–243.

[118] Y. Guangqiang, “LARGE-SCALE MAGNETORHEOLOGICAL FLUID DAMPER FOR VIBRATION MITIGATION: MODELING, TESTING AND CONTROL,” Ph.D. thesis, University of Notre Dame, Indiana, 2001.

[119] Z. Chen, “SEMIACTIVE VIBRATION CONTROL USING SELF-SENSING MAGNETORHEOLOGICAL (MR) DAMPERS,” Ph.D. thesis, Hong Kong Polytechnic University, 2011.

[120] C.-C. Chang and P. Roschke, “Neural Network Modeling of a Magnetorheological Damper,” *J. Intell. Mater. Syst. Struct.*, vol. 9, no. 9, pp. 755–764, Sep. 1998.

[121] D. H. Wang and W. H. Liao, “Modeling and control of magnetorheological fluid dampers using neural networks,” *Smart Mater. Struct.*, vol. 14, no. 1, pp. 111–126, Feb. 2005.

[122] M. Cao, K. W. Wang, and K. Y. Lee, “Scalable and Invertible PMNN Model for MagnetoRheological Fluid Dampers,” *J. Vib. Control*, vol. 14, no. 5, pp. 731–751, May 2008.

[123] M. J. L. Boada, J. A. Calvo, B. L. Boada, and V. Díaz, “Modeling of a magnetorheological damper by recursive lazy learning,” *Int. J. Non. Linear. Mech.*, vol. 46, pp. 479–485, 2011.

[124] J. S. Won and M. Sunwoo, “Fuzzy modelling approach to magnetorheological

dampers: Forward and inverse model," *Proc. Inst. Mech. Eng. Part I J. Syst. Control Eng.*, vol. 223, no. 8, pp. 1055–1066, 2009.

[125] H. Wang, "Modeling of Magnetorheological Damper Using Neuro-Fuzzy System," Springer, Berlin, Heidelberg, 2009, pp. 1157–1164.

[126] F. Imaduddin, S. A. Mazlan, Ubaidillah, M. H. Idris, and I. Bahiuddin, "Characterization and modeling of a new magnetorheological damper with meandering type valve using neuro-fuzzy," *J. King Saud Univ. - Sci.*, vol. 29, no. 4, pp. 468–477, Oct. 2017.

[127] A. Sarrafan, S. H. Zareh, A. A. A. Khayyat, and A. Zabihollah, "Neuro-fuzzy control strategy for an offshore steel jacket platform subjected to wave-induced forces using magnetorheological dampers," *J. Mech. Sci. Technol.*, vol. 26, no. 4, pp. 1179–1196, Apr. 2012.

[128] P. W. Nugroho, W. Li, H. Du, G. Alici, and J. Yang, "An Adaptive Neuro-Fuzzy Hybrid Control Strategy for a Semiactive Suspension with Magneto-Rheological Damper," *Adv. Mech. Eng.*, vol. 6, p. 487312, Jan. 2014.

[129] S.-B. Choi, S.-K. Lee, and Y.-P. Park, "A HYSTERESIS MODEL FOR THE FIELD-DEPENDENT DAMPING FORCE OF A MAGNETORHEOLOGICAL DAMPER," *J. Sound Vib.*, vol. 245, no. 2, pp. 375–383, Aug. 2001.

[130] A. Leva and L. Piroddi, "NARX-based technique for the modelling of magneto-rheological damping devices," *Smart Mater. Struct.*, vol. 11, no. 1, pp. 79–88, Feb. 2002.

[131] X. Song, M. Ahmadian, and S. C. Southward, "Modeling Magnetorheological Dampers with Application of Nonparametric Approach," *J. Intell. Mater. Syst. Struct.*, vol. 16, no. 5, pp. 421–432, May 2005.

[132] H.-B. Yun and S. F. Masri, "Stochastic change detection in uncertain nonlinear systems using reduced-order models: system identification," *Smart Mater. Struct.*, vol. 17, no. 1, p. 015040, Feb. 2008.

[133] K.-J. Kim, C.-W. Lee, and J.-H. Koo, "Design and modeling of semi-active squeeze film dampers using magneto-rheological fluids," *Smart Mater. Struct.*, vol. 17, no. 3, p. 035006, Jun. 2008.

[134] M. Mori and A. Sano, "Local modeling approach to vibration control by MR damper," *SICE 2004 Annu. Conf.*, vol. 3, pp. 2572–2577, 2004.

[135] K. Hudha, H. Jamaluddin, P. M. Samin, and R. A. Rahman, "Non-parametric linearised data-driven modelling and force tracking control of a magnetorheological damper," *Int. J. Veh. Des.*, vol. 46, no. 2, p. 250, 2008.

[136] Johnson Matthey Piezoproducts Bahnhofstraße 43, "Data Sheet Piezoceramic Trimorph Bending Actuator, Part No. 427.0085.11Z,, D-96254 Redwitz." .

[137] H. Azangbebil, S. S. Djokoto, and M. Agelin-Chaab, "Experimental and numerical studies of a soft impact piezoelectric energy harvesting using an MR fluid," *IEEE*

Sens. J., pp. 1–1, 2020.

[138] M. Nagurka and S. Huang, "A mass-spring-damper model of a bouncing ball," in *Proceedings of the American Control Conference*, 2004, vol. 1, no. 3, pp. 499–504.

[139] Y. Liao and H. A. Sodano, "Modeling and comparison of bimorph power harvesters with piezoelectric elements connected in parallel and series," *J. Intell. Mater. Syst. Struct.*, vol. 21, no. 2, pp. 149–159, 2010.

[140] "Lord Corporation, MRF-140CG, Magneto-Rheological Fluid," *Lord product selector guide: lord magnetorheological fluids*, 2014.

[141] J. D. Carlson, "MR fluids and devices in the real world," *Int. J. Mod. Phys. B*, vol. 19, no. 7–9, pp. 1463–1470, 2005.

[142] S. R. Hong, S. B. Choi, W. J. Jung, and W. B. Jeong, "Vibration isolation of structural systems using squeeze mode ER mounts," *J. Intell. Mater. Syst. Struct.*, vol. 13, no. 7–8, pp. 421–424, 2002.

[143] M. R. Jolly and J. D. Carlson, "Controllable Squeeze Film Damping Using Magnetorheological Fluid," in *5th International Conference on New Actuators*, 1996, pp. 333–336.

[144] P. F. Beer, E. R. Johnson, and T. J. Dewolf, *Mechanics of Materials*, 4th ed. New York: McGraw Hill, 2006.

[145] W. G. Ali and S. W. Ibrahim, "Power Analysis for Piezoelectric Energy Harvester," *Energy Power Eng.*, vol. 04, no. 06, pp. 496–505, 2012.

[146] S. Kolekar, K. Venkatesh, J. S. Oh, and S. B. Choi, "The tenability of vibration parameters of a sandwich beam featuring controllable core: Experimental investigation," *Adv. Acoust. Vib.*, vol. 2017, 2017.

[147] M. Gorlatova, J. Sarik, G. Grebla, M. Cong, I. Kymissis, and G. Zussman, "Movers and Shakers: Kinetic Energy Harvesting for the Internet of Things," *IEEE J. Sel. Areas Commun.*, vol. 33, no. 8, pp. 1624–1639, Aug. 2015.

[148] R. Dauksevicius *et al.*, "Nonlinear piezoelectric vibration energy harvester with frequency-tuned impacting resonators for improving broadband performance at low frequencies," *Smart Mater. Struct.*, vol. 28, no. 2, p. 25025, 2019.

[149] D. Žižys, R. Gaidys, V. Ostaševičius, and B. Narijauskaitė, "Vibro-shock dynamics analysis of a tandem low-frequency resonator—high-frequency piezoelectric energy harvester," *Sensors (Switzerland)*, vol. 17, no. 5, pp. 1–21, 2017.